microorganisms

MDPI

Article

Comparative Genomics of a Root- and Soil-Associated *Pantoea* clade: Phosphorus Mobilization and Homeostasis Pathways

José Luis Aguirre-Noyola [1,*], Gustavo Cuaxinque-Flores [2], Lorena Jacqueline Gómez-Godínez [1], Jorge David Cadena-Zamudio [1], Marco A. Ramírez-Mosqueda [1] and Alma Armenta-Medina [1]

[1] Centro Nacional de Recursos Genéticos, Instituto Nacional de Investigaciones Forestales, Agrícolas y Pecuarias (INIFAP), Boulevard de la Biodiversidad No. 2498, Rancho las Cruces, Tepatitlán de Morelos 47600, Mexico

[2] Centro de Ciencias Genómicas, Universidad Nacional Autónoma de México, Av. Universidad S/N, Chamilpa, Cuernavaca 62210, Mexico

* Correspondence: aguirre.jose@inifap.gob.mx

Abstract

Phosphorus is one of the nutrients that most limit agricultural productivity, because most of it occurs in precipitated inorganic or organic forms that plants cannot take up directly. Phosphorus-mobilizing bacteria are an alternative to chemical fertilization. In *Pantoea brenneri*, this capacity has been described only in strains from soil, so it is not known whether it extends to strains associated with plant roots. This study describes the phosphorus mobilization and homeostasis pathways of *P. brenneri* ZM06, a phosphate-solubilizing strain from the maize rhizoplane (Pepitilla landrace). Its genome was sequenced with Illumina and assigned taxonomically by overall genome relatedness indices and phylogenomics. It was then compared with those of diverse *Pantoea* species through pangenomics and mining of genes involved in plant growth promotion, phosphorus mobilization and root colonization. *P. brenneri ZM06* (4.79 Mb, 56.0% G+C) was placed within *P. brenneri* and, together with four soil strains, formed the Root- and Soil-associated *Pantoea* clade (ANI > 99%, AAI > 99%, dDDH > 95%). The genome of *P. brenneri ZM06* encodes the Gcd-PQQ system, three gluconate 2-dehydrogenase loci, two HAP-family phytases, an alkaline phosphatase, the Ugp system, a C-P lyase cluster lacking *phnO*, two *pst* loci, one complete (*pstSCAB-phoU*) and one comprising *pstCAB* without a colocated *pstS*, and the polyphosphate pathway. These genes and their organization were conserved in all five strains, with a single difference in a second copy of *appA*, as were the colonization determinants. The genetic potential for phosphorus mobilization was conserved in the five strains, independently of isolation source, so strain selection for biotechnological applications should be based on the expression of these mobilization and homeostasis pathways rather than on the presence of the genes.

Keywords: *Pantoea brenneri*; phosphate solubilization; phytase; maize; *Zea mays*

Check for updates

Academic Editor: Rainer Borriss

Received: 25 October 2026
Revised: 16 November 2026
Accepted: 24 November 2026
Published: 26 November 2026

Copyright: © 2026 by the authors. Licensee MDPI, Basel, Switzerland. This article is an open access article distributed under the terms and conditions of the Creative Commons Attribution (CC BY) license.

1. Introduction

Phosphorus (P) is one of the nutrients that most limit agricultural productivity [1,2]. Although it is abundant in soil, most of it is unavailable to plants, which only take up soluble ionic forms such as $H_2PO_4^-$ and HPO_4^{2-} [1]. In acidic soils, phosphate is adsorbed onto iron (Fe) and aluminum (Al) oxides and secondary clay minerals [3]. In contrast, in alkaline and calcareous soils, it precipitates with calcium (Ca) and magnesium (Mg) as dicalcium phosphate ($CaHPO_4$) and octacalcium phosphate ($Ca_8H_2(PO_4)_6{\cdot}5H_2O$) [4]. Another important fraction is incorporated into organic compounds, which must be mineralized before

plants can use them [1]. For these reasons, agriculture relies on chemical fertilization, which depends on phosphate rock, a nonrenewable resource, and whose excessive application is associated with soil degradation [1,5].

Various soil microorganisms can mobilize these forms of phosphorus through complementary pathways [1,2]. Inorganic phosphorus is solubilized mainly by organic acids, particularly gluconic acid ($C_6H_{12}O_7$). This acid is produced in the periplasm by pyrroloquinoline quinone (PQQ)-dependent glucose dehydrogenase (*gcd*), with PQQ synthesis encoded by the *pqq* operon [6,7], and it can be oxidized to 2-ketogluconic acid ($C_6H_{10}O_7$), a more effective acidulant, by gluconate 2-dehydrogenase [8]. Organic phosphorus, in contrast, is mineralized by acid and alkaline phosphatases and phytases, whereas phosphonates are used through the carbon–phosphorus lyase (C-P lyase) complex, encoded by the *phn* genes [1,2]. These pathways are coupled to cellular phosphorus homeostasis. The PhoR-PhoB system, together with the high-affinity transporter PstSCAB, senses phosphate limitation and activates the Pho regulon, which induces phosphatases and phytases [9]. Excess phosphorus is stored as polyphosphate (polyP) by polyphosphate kinases (encoded by *ppk*) and mobilized by exopolyphosphatases (encoded by *ppx*) [10,11].

Phosphorus is particularly relevant for maize (*Zea mays* L.) yield, and bacteria have been used as a strategy to increase the bioavailability and uptake of this element [2]. In P-deficient agricultural soils, inoculation with phosphate-solubilizing rhizobacteria, including *Rhodococcus* sp. and *Arthrobacter nicotinovorans*, promoted plant growth [12]. Likewise, application of *Pseudomonas tolaasii* increased grain yield by 44% and P content by 56% relative to the uninoculated control [13]. In Brazil, coinoculation with *Bacillus megaterium* B119 and *B. subtilis* B2084 increased grain yield by up to 24%, in addition to increasing P accumulation in the grain [14]. Even so, inoculation has not consistently reduced the use of chemical fertilizers, because its efficacy varies with the strain and the soil, and the mechanisms of phosphorus mobilization remain poorly understood [15].

Among the bacterial genera associated with maize is *Pantoea* (Enterobacterales), whose members colonize plant tissues and display plant growth-promoting traits [16,17]. The genes associated with these traits are widely distributed across the genus, even in phytopathogenic and clinical lineages, so their presence or absence is not sufficient to define the lifestyle of a strain [16,18]. *Pantoea brenneri* was described from human clinical isolates, but it also has agrobiotechnological potential, since it solubilizes inorganic phosphates, hydrolyzes phytate, and promotes plant growth [19,20]. The genomes of four soil-isolated, phytase-producing strains of this species have been sequenced [21], and, to our knowledge, the genome of a maize root-associated strain has not been described. It is therefore not known whether the phosphorus mobilization repertoire of this species is conserved across it or restricted to soil-adapted strains. The genome of a strain from the roots makes that question testable, which is the contribution expected here rather than a further inventory of known genes.

Therefore, the aim of this work was to analyze the genome of *Pantoea* strain ZM06, isolated from maize roots, and to evaluate, through comparative genomics, the conservation of phosphorus mobilization and homeostasis pathways among the strains of the Root- and Soil-associated *Pantoea* clade. In addition, this work sought to identify potential genetic determinants involved in the plant–bacteria interaction. It was hypothesized that the genetic potential for phosphorus mobilization and homeostasis is conserved within the clade, regardless of isolation source, and that genomic variation among strains is concentrated in the accessory genome. Whether the determinants associated with root colonization follow the same pattern of conservation was examined as part of the genomic comparison.

2. Materials and Methods

2.1. Strain Isolation and Selection

P. brenneri ZM06 was isolated from native maize plants of the Pepitilla landrace collected in Chilacachapa, municipality of Cuetzala del Progreso, Guerrero, Mexico (18.273260° N, 99.760933° W). Three plants were removed with the root ball at the V6 phenological stage, and the roots were gently shaken to remove loosely adhering soil. In the laboratory, the roots of the three plants were pooled, and 10 g of fine roots was washed three times with sterile distilled water to remove rhizosphere soil and transferred to a flask containing 90 mL of sterile saline solution (0.85% NaCl) supplemented with 0.1% Tween 20. The suspension was sonicated three times for 30 s, with 20 s intervals, to detach cells adhered to the root surface. The rhizoplane suspension was serially diluted to 10^{-4} in sterile saline solution and spread-plated onto Pikovskaya medium (glucose 10 g L^{-1}, $Ca_3(PO_4)_2$ 5 g L^{-1}, $(NH_4)_2SO_4$ 0.5 g L^{-1}, NaCl 0.2 g L^{-1}, $MgSO_4 \cdot 7H_2O$ 0.1 g L^{-1}, KCl 0.2 g L^{-1}, yeast extract 0.5 g L^{-1}, $MnSO_4$ 0.002 g L^{-1}, $FeSO_4$ 0.002 g L^{-1}, and agar 15 g L^{-1}, pH 7) [22]. Plates were incubated at 30 °C for 7 days. Screening was directed at colonies producing a clear solubilization halo rather than at the recovery of the culturable microbiota. Two halo-forming morphotypes were obtained, and their solubilization index (SI) was determined in three replicates and expressed as the mean ± standard deviation. The index was calculated as SI = (C + H)/C, where C is the colony diameter (mm) and H is the diameter of the solubilization halo (mm). The solubilization indices of the two morphotypes were compared with Student's *t*-test. Strain ZM06 was selected for genome sequencing because it showed the higher index.

2.2. DNA Extraction, Sequencing, Assembly, and Functional Annotation

Genomic DNA of strain ZM06 was extracted with the Quick-DNA Fungal/Bacterial Miniprep Kit (Zymo Research, Irvine, CA, USA). DNA was sent to Macrogen Inc. (Seoul, Republic of Korea), where libraries were constructed with the TruSeq Nano DNA protocol (Illumina, San Diego, CA, USA), with an approximate insert size of 350 bp, and sequenced on an Illumina NovaSeq 6000 platform (Illumina, San Diego, CA, USA) (2 × 150 bp). Raw read quality was assessed with FastQC v0.12.1 [23]. Sequencing yielded 9,375,398 read pairs, which were trimmed with Trim Galore v0.6.10 [24] in paired-end mode, with automatic adapter detection and a Phred quality threshold of 30. Pairs with a read shorter than 20 bp were discarded, leaving 9,159,215 read pairs (97.69%). The reads were assembled de novo with Unicycler v0.5.1 [25] in short-read mode with default parameters (unicycler -1 R1 -2 R2 -o out -t 20), which runs SPAdes v4.2.0 with multiple k-mer sizes, cleans the assembly graph and removes low-depth contigs. Contigs shorter than 200 bp were discarded. Genome completeness and contamination were estimated with CheckM v1.2.2 using the lineage_wf workflow, which selected the Enterobacteriaceae lineage-specific marker set (UID5124) [26]. Genome coverage was calculated with BBMap v39.25 [27]. Gene prediction and functional annotation were performed with Bakta v1.11.0 [28]. COG functional categories were assigned with COGclassifier v1.0.5, and the genome map was generated with MGCplotter v1.0.1 and pyCirclize v0.2.1.

The assembly was screened with ABRicate v1.2.0 (BLAST+ v2.17.0; identity ≥ 70%, coverage ≥ 60%) against CARD, the NCBI AMR reference gene database, ResFinder, MEGARes and ARG-ANNOT for resistance determinants, and against VFDB, Victors and *Escherichia coli* VF for virulence factors [29].

2.3. Taxonomic Assignment and Comparative Genomics

Initial taxonomic assignment was performed with the Genome Taxonomy Database Toolkit (GTDB-Tk v2.6.1) against the complete GTDB R226 database, using the classify_wf workflow on the Galaxy server (version 2.6.1+galaxy0) [30]. A set of reference genomes

downloaded from NCBI RefSeq (September 2026) was included, and their characteristics are shown in Supplementary Table S1. Average nucleotide identity (ANI) between strains was calculated from genome alignments with PyANI v0.3.0-alpha using NUCmer v3.1 [31], and average amino acid identity (AAI) was estimated with CompareM v0.1.2. In silico DNA-DNA hybridization (dDDH) analyses were performed on the Type (Strain) Genome Server (TYGS) [32,33]. Homologous gene clusters of the pangenome were identified with GET_HOMOLOGUES v14112024 [34]. The BDBH, COGtriangles, and OrthoMCL algorithms were used with a minimum coverage of 75% and an E-value of 1×10^{-5}, and genes were classified as core, soft core, shell, and cloud with the auxiliary script parse_pangenome_matrix.pl. Phylogenomic markers were selected with GET_PHYLOMARKERS v2.8.1.4 [35] from the 1684 single-copy orthologous groups (OGs) of the strict core. Successive filters removed 643 alignments that failed the test of stationarity, reversibility and homogeneity of the substitution process; 136 with evidence of recombination by the Phi permutation test; 31 gene trees that were trivial or topological outliers under the kernel density estimation filter; and 464 with low median bipartition support. The 410 retained markers were concatenated for the phylogenomic inference. The OGs exclusive to *P. brenneri* ZM06 were annotated with eggNOG-mapper v2.1 [36] against the eggNOG v5.0 database [37]. The species tree was inferred by maximum likelihood from the concatenated supermatrix of these markers with IQ-TREE v2.3.1 [38], using the LG+F+R3 substitution model selected by ModelFinder [39]. Based on this tree, a Root- and Soil-associated *Pantoea* clade was delimited as a well-supported clade comprising the four *P. brenneri* strains isolated from soil and strain ZM06 from maize roots. The clade was not delimited from tree topology alone. It was defined as the set of strains that exceed the species boundary against ZM06, based on ANI and AAI values > 99%, dDDH values > 95%, and phylogenetic support values of aBayes ≥ 0.95 [40,41] and UFBoot > 95% [42].

2.4. In Silico Prediction of Plant Growth-Promoting Traits

Proteins of the Root- and Soil-associated *Pantoea* clade were predicted with Prodigal v2.6.3 [43] and searched against the plant growth-promoting trait database (PGPT-db) of PLaBAse [44] following the PGPg_finder workflow [45] with DIAMOND v2.2.8 [46], using a minimum identity of 40%, query coverage of 70%, and an E-value ≤ 1×10^{-10}. Detected genes were classified according to their direct effects (biofertilization, production of phytohormones and plant signals, and bioremediation) or indirect effects (plant colonization, competitive exclusion, stress control and biocontrol, and stimulation of the plant immune response), together with an eighth category comprising putative functions. Because the PGPT ontology is hierarchical, a protein may be assigned to more than one subcategory. Plant–bacteria interaction factors were identified by comparing the proteomes against the PIFAR (Plant–bacteria Interaction Factors Resource) protein collection [47], which includes genes associated with the use of plant-derived substrates, motility and chemotaxis, surface adhesion, root colonization, plant cell wall degradation, and adaptation to the plant immune system.

2.5. Genome Mining of Phosphorus Mobilization, Transport, and Storage Genes

Genes associated with phosphorus solubilization, mineralization, transport, and storage were identified through BLASTp v2.17.0 [48] searches of the Bakta-predicted proteomes against a curated database of reference proteins obtained from UniProtKB, and are listed with their accession numbers, source organisms and EC numbers in Supplementary Table S2. Searches were performed with strict thresholds (E-value ≤ 1×10^{-15}, sequence identity ≥ 30%, and alignment coverage ≥ 70%). Representative genes of the main phosphorus metabolism pathways were included, covering gluconic acid synthesis, oxidation

of gluconate to 2-ketogluconate, acid and alkaline phosphatases, phytases, glycerophosphodiester phosphodiesterases, the C-P lyase system for phosphonate degradation, high- and low-affinity inorganic phosphate transport systems, glycerol-3-phosphate transport (*ugp*), the Pho regulon, and polyphosphate metabolism. The organization of phosphorus gene clusters was obtained from the coordinates of the Bakta GFF3 file (Supplementary Table S3), including adjacent genes, and their conservation was compared with clinker v0.0.32 [49] and CORASON [50].

3. Results

3.1. Isolation and Selection of Strain ZM06

Two colony morphotypes from the rhizoplane produced a clear solubilization halo on Pikovskaya medium after 7 days at 30 °C. The colonies of the more abundant morphotype were round, convex and smooth, with entire margins and pale yellow pigmentation. Its solubilization index was 2.5 ± 0.11, against 1.3 ± 0.14 for the second morphotype ($p < 0.001$). This strain, designated ZM06, was selected for genome sequencing (Figure 1).

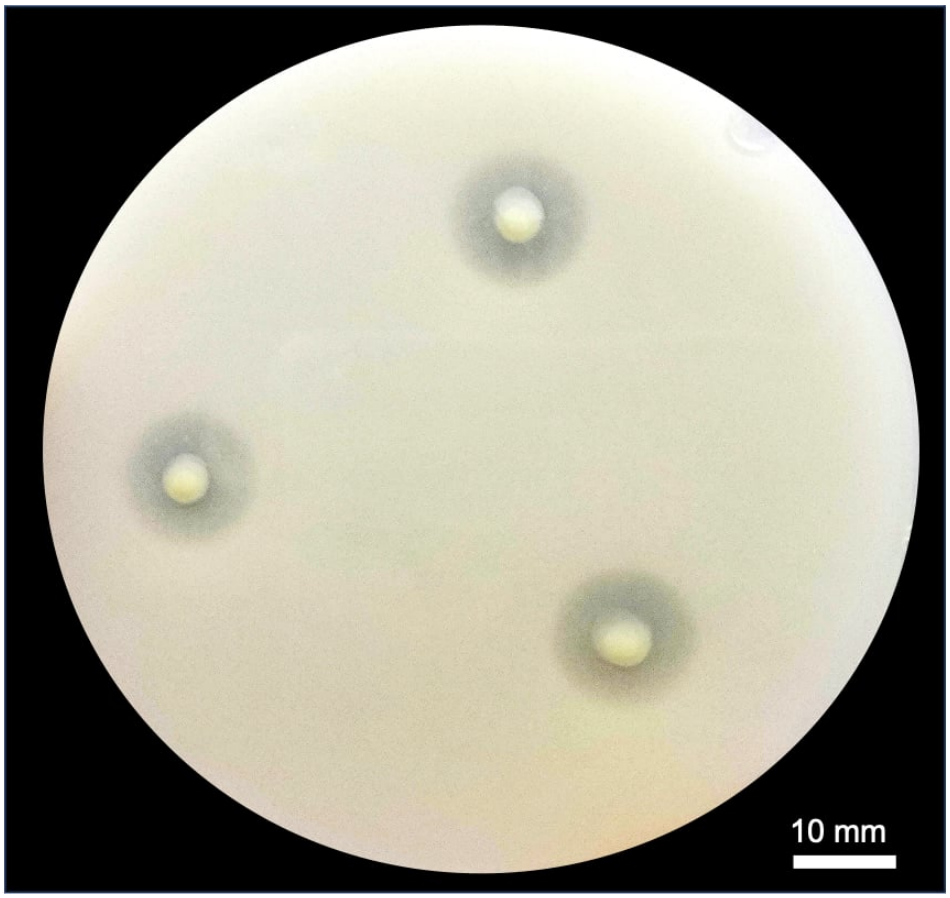


Figure 1. Colonies of *Pantoea brenneri* ZM06 on Pikovskaya medium after 7 days at 30 °C, surrounded by solubilization halos. Scale bar, 10 mm.

3.2. Taxonomic Identity and Genome Features

According to the GTDB, strain ZM06 was classified as *Pantoea*, and the closest reference genome was that *of P. brenneri* LMG 5343^{T}. The assembly of the ZM06 genome yielded 60 contigs with a total length of 4,794,302 bp, a G+C content of 56.0%, and an N50 of 279,510 bp (Figure 2a, Table 1). Genome completeness reached 100% and contamination was 0%. A mean coverage of 582× was obtained, with 100% of bases covered.

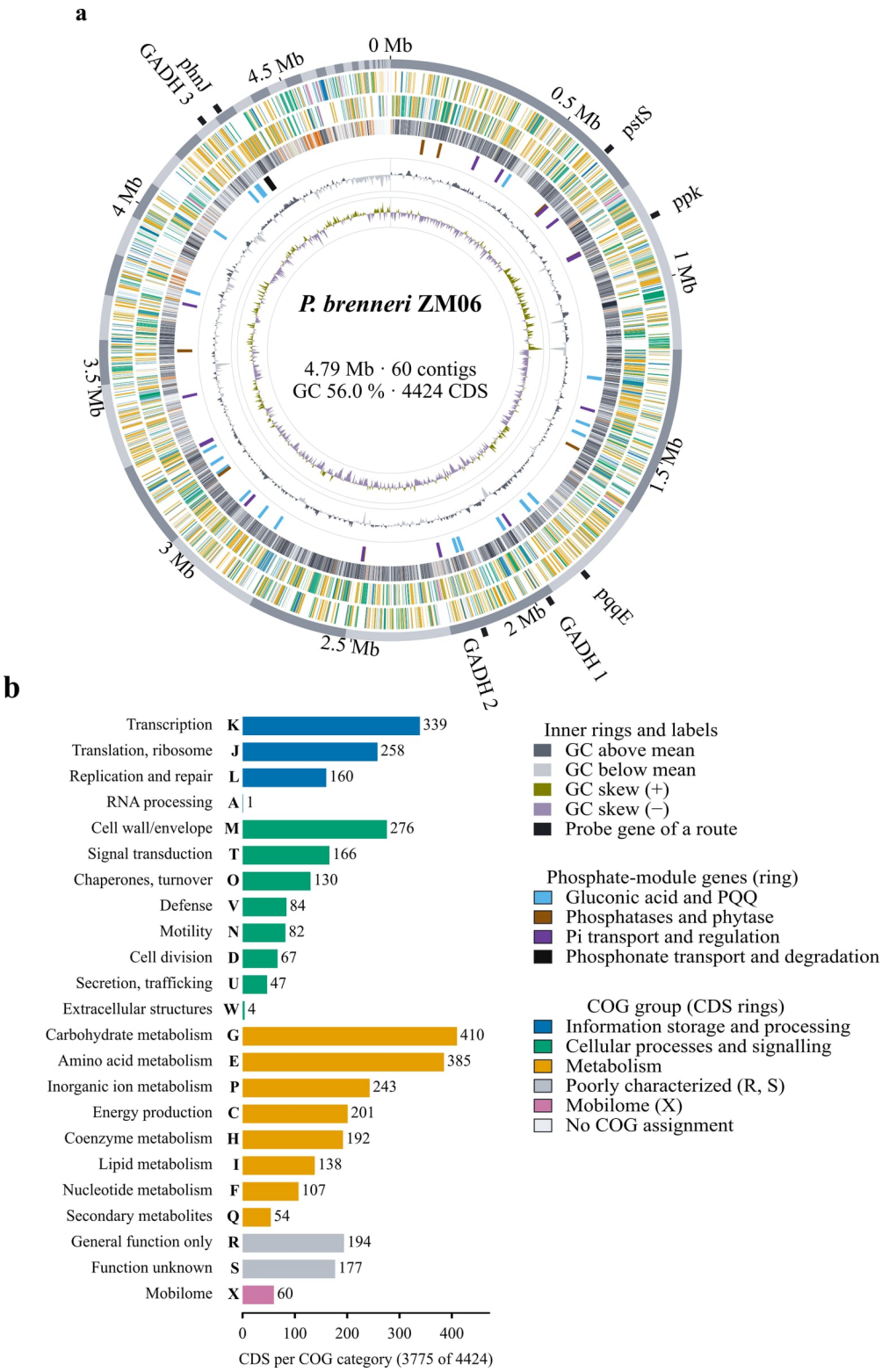


Figure 2. Genome of *P. brenneri* ZM06. (**a**) Circular map showing, from outside to inside, the contigs, the coding sequences on the forward and reverse strands colored by COG functional group, the genes of the phosphorus mobilization and homeostasis clusters, the G+C content and the GC skew. (**b**) Number of coding sequences per COG category (K, J, L, A, M, T, O, V, N, D, U, W, G, E, P, C, H, I, F, Q, R, S, X).

Table 1. Assembly and annotation statistics of the *P. brenneri* ZM06 genome.

Genome Feature *	Value
Sequencing	
Raw read pairs	9,375,398
Read pairs retained after trimming	9,159,215
Mean coverage	582×
Assembly	
Total length (bp)	4,794,302
Contigs	60
N50 (bp)	279,510
G+C content (%)	56.0
Completeness (%)	100
Contamination (%)	0
Annotation	
Coding sequences (CDSs)	4424
CDS assigned to a COG category	3775
Pseudogenes	6
tRNA genes	72
rRNA genes	4
Data availability	
Assembly accession	GCA_062061765.1

* Annotation values correspond to the Bakta annotation and coverage was estimated with BBMap. Completeness and contamination were estimated with CheckM v1.2.2.

Functional annotation predicted 4424 coding sequences (CDSs), 6 pseudogenes, 72 tRNAs, and 4 rRNAs. Of the total CDSs, 3775 (85.3%) were assigned to a COG category (Figure 2b). Among the functional categories, the largest group corresponded to metabolism (1730 CDSs, 45.8%), mainly carbohydrate transport and metabolism (G: 410) and amino acid transport and metabolism (E: 385), followed by inorganic ion metabolism (P: 243), energy production and conversion (C: 201), and coenzyme metabolism (H: 192). Cellular processes and signaling comprised 856 CDSs (22.7%), including cell wall and envelope (M: 276), signal transduction (T: 166), chaperones and protein turnover (O: 130), defense mechanisms (V: 84), motility (N: 82), cell division (D: 67), and secretion and vesicular trafficking (U: 47). Information storage and processing comprised 758 CDSs (20.1%), mainly transcription (K: 339), translation and ribosome (J: 258), and replication and repair (L: 160). The general or unknown function categories (R and S) represented 371 CDSs (9.8%), and the mobilome (X), 60 CDS (1.6%).

No acquired antimicrobial resistance genes were detected in the genome of strain ZM06. The hits recovered corresponded to chromosomal efflux systems intrinsic to the *Enterobacteriaceae*, including AcrAB, MdtABC, OqxAB and KpnEF. Hits against the virulence databases corresponded to flagellar, enterobactin biosynthesis and regulatory genes, with no toxin genes and no type III secretion system.

3.3. Identification of a Root- and Soil-Associated Pantoea clade

The ANI between ZM06 and the type strain LMG 5343^T was 99.29%, the AAI 98.88% and the dDDH 93.3%, all above the thresholds that delimit a prokaryotic species. After *P. brenneri*, the species closest to ZM06 were *P. conspicua* (ANI of 91.43%) and *Candidatus Pantoea astica* (ANI of 91.41%) (Supplementary Tables S4 and S5).

ANI and AAI values among *P. brenneri* ZM06 and the four soil strains were above the species threshold (Figure 3). The dDDH of ZM06 was 95.4% against strains 3.1, 3.6.1 and *Pantoea* sp. 3.5.1, and 96.4% against *P. brenneri* 3.5.2 (Supplementary Table S6). The five strains

formed a well-supported group in the phylogenomic tree (aBayes ≥ 0.95, UFBoot ≥ 95% from 1000 replicates; Figure 4), referred to here as the Root- and Soil-associated *Pantoea* clade. The pangenome comprised 13,474 OGs (Figure 5a). Of these, 1756 (13.0%) formed the core, 660 (4.9%) the soft core, 3382 (25.1%) the shell, and 7676 (57.0%) the cloud (Figure 5b). On the other hand, the strict core genome consisted of 1684 single-copy OGs present in all 37 genomes included, which formed the basis of the phylogenomic analysis (Figure 5c). Accumulation curves showed that the pangenome is open, since each added genome contributes on average approximately 79 new genes (Figure 5d), whereas the core genome gradually decreases to 1756 OGs (Figure 5e). The Heaps' law exponent was $\alpha = 0.59$ (95% confidence interval, 0.53 to 0.66), lower than 1, which confirms that the pangenome grows with each added genome (Figure 5f). We found 211 OGs exclusive to *P. brenneri* ZM06 (Figure 5g, Supplementary Table S7). Most of this fraction lacks a functional assignment: 115 groups returned no COG category and 34 were assigned to category S (function unknown). The remaining 62 groups are distributed across 18 categories. The largest is replication, recombination and repair, with 21 groups that include eleven IS3 family and one Tn3 family transposases and one integrase. Three groups are assigned to cell motility, three to defense mechanisms, among them the restriction endonucleases EcoRII and NgoMIV, and three to inorganic ion transport and metabolism (P), which encode heavy-metal P-type ATPases and arsenite efflux permeases, none involved in phosphate transport.

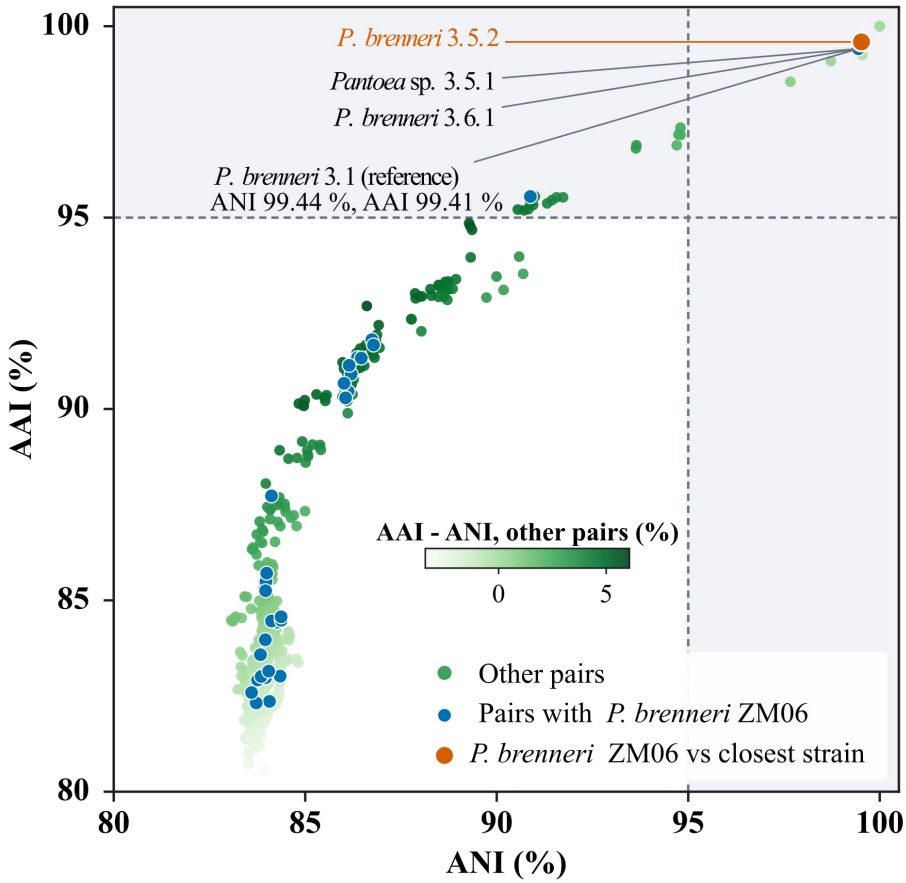


Figure 3. ANI versus AAI for all pairs of the *Pantoea* genomes analyzed. Green dots correspond to pairs between reference genomes, with color intensity according to the AAI − ANI difference. Dashed lines indicate the 95% species threshold for ANI and AAI.

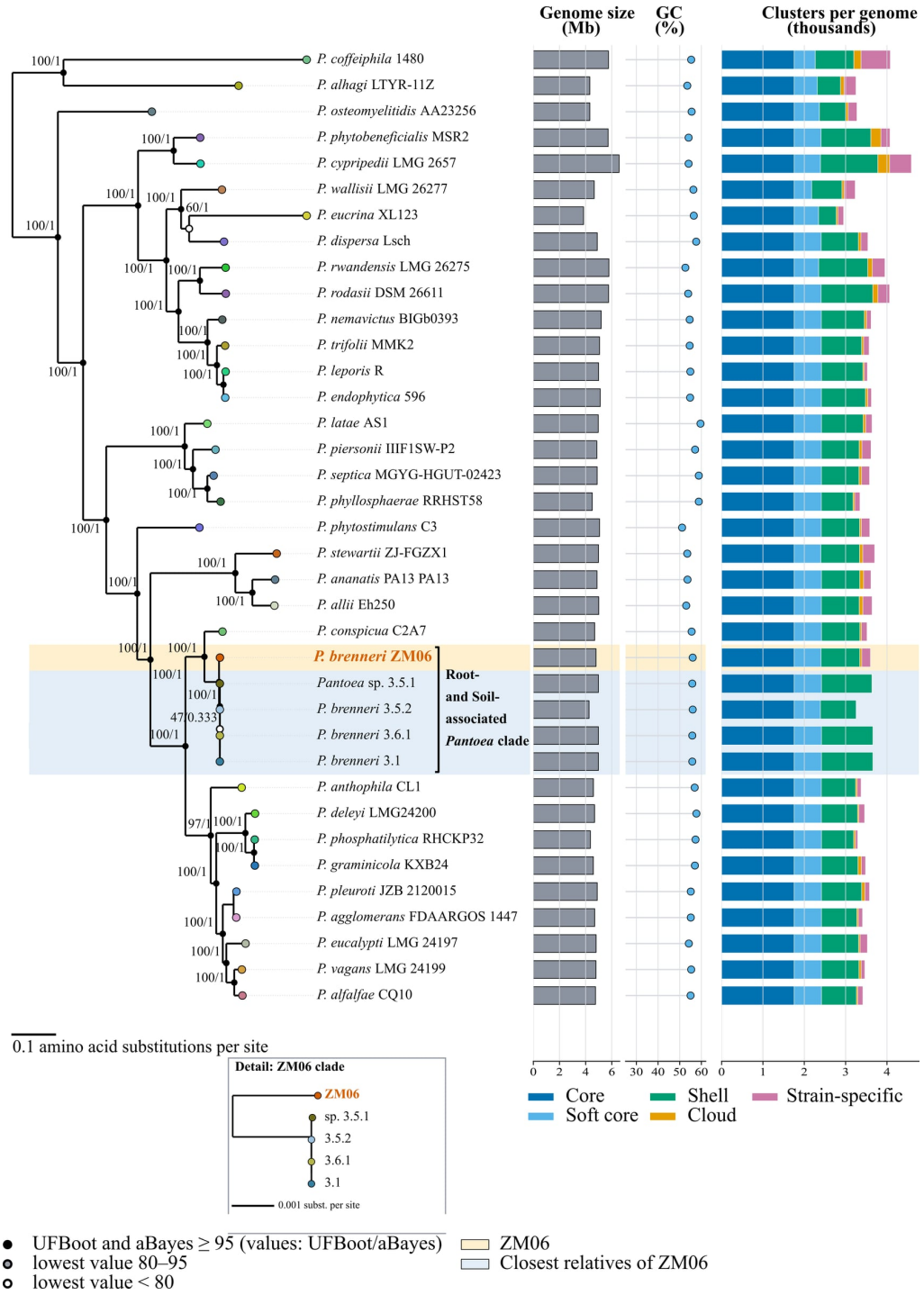


Figure 4. Phylogenomic tree of the *Pantoea* genomes analyzed. The tree was inferred by maximum likelihood from 410 single-copy markers with the LG+F+R3 model. Symbols indicate node support (UFBoot/aBayes), and the panels show genome size, GC content, and OG composition by pangenome category. The shaded area corresponds to the Root- and Soil-associated *Pantoea* clade.

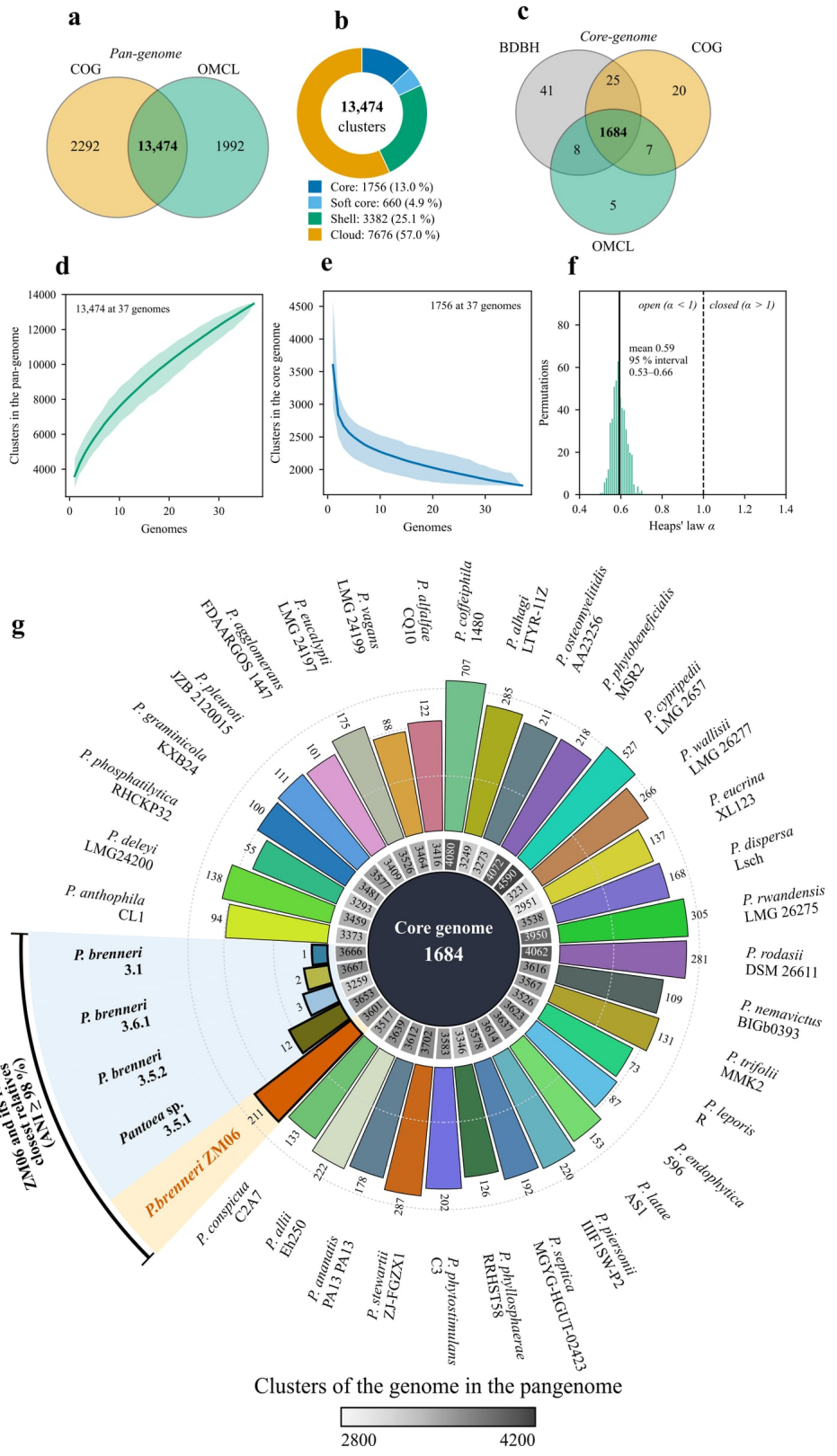


Figure 5. Pangenome and core genome of the *Pantoea* genomes analyzed. (**a**) Venn diagram of pangenome OGs from COGtriangles and OrthoMCL. (**b**) Pangenome composition by category (core, soft core, shell, cloud). (**c**) Venn diagram of the core genome from BDBH, COGtriangles and OrthoMCL. (**d**) Pangenome growth and (**e**) core genome decay over 500 permutations of genome order, with the mean as a line and the 95% interval as a band. (**f**) Distribution of the Heaps' law exponent α, with the dotted line at α = 1 and α < 1 indicating an open pangenome. (**g**) Accessory genome per strain, with the core genome at the center, the OGs of each genome in the inner ring and strain-specific OGs in the bars. The Root- and Soil-associated *Pantoea* clade is highlighted.

3.4. Genes Associated with Phosphorus Mobilization

In terms of solubilization, the genome of *P. brenneri* ZM06 encodes a two-step direct periplasmic glucose oxidation pathway (glucose to gluconate and gluconate to 2-ketogluconate). The first step is represented by pyrroloquinoline quinone (PQQ)-dependent glucose dehydrogenase (*gcd*) (Figure 6a) and by the biosynthesis genes of this cofactor, organized in the pqqABCDEF cluster (Figure 6b). A gluconolactonase (gnl) and the gluconate transporters *gntP*, *gntT*, and *gntU* were also identified. The second step corresponds to the oxidation of gluconate to 2-ketogluconate, for which three gluconate 2-dehydrogenase (GADH) loci were found, each with the small, flavoprotein, and cytochrome c subunits in contiguous position (Figure 6c–e). Each subunit was assigned by homology to the corresponding subunit of the characterized GADH of *P. cypripedii* (UniProt O34213, O34214 and O34215). A 2-ketogluconate reductase was also identified, carrying the Pfam domains PF00389 and PF02826. The remaining genes identified by genome mining were assigned to organic acid metabolism (citric, malic, succinic, lactic, and acetic acids) and were not considered specific solubilization determinants.

As for organic phosphorus mineralization, two enzymes of the histidine acid phosphatase family, the group to which bacterial phytases belong, were identified. The first is a bifunctional glucose-1-phosphatase with inositol phosphatase activity (*agp*), and the second is an AppA-type 3-phytase, adjacent to an inositol monophosphatase. A gene encoding an alkaline phosphatase (phoA) was also detected. The genome also encodes the cytoplasmic glycerophosphodiester phosphodiesterase ugpQ and the glycerol-3-phosphate transport system ugpBAEC (Figure 6g), which together enable the use of phospholipid-derived phosphodiesters. For the use of phosphonates as a phosphorus source, the genes of the C-P lyase system were found, organized in a contiguous 14-gene cluster in which the components of the catalytic complex and their accessory proteins (*phnFGHIJKLMNP*) precede those of the transporter (*phnCDE*, with two copies of *phnE*) (Figure 6h). No *phnO* was detected.

For phosphate transport and homeostasis, *P. brenneri ZM06* has two high-affinity transport systems. The first corresponds to the *pstSCAB-phoU* operon (Figure 6i), whereas the second consists of *pstCAB* and is located adjacent to the *ppx* and *ppk1* genes (Figure 6j). This second locus lacks a colocated *pstS*. A second copy of *pstS* is located next to the PhoR-PhoB two-component system, which regulates the response to phosphate limitation, in the same region as the *appA* phytase (Figure 6f). Other members of the Pho regulon were also identified, such as *phoH* and psiE, the phosphate limitation-inducible porin phoE, and the low-affinity transporters pitA and yjbB. Regarding the genes involved in polyphosphate synthesis and degradation, the genome encodes a polyphosphate kinase (ppk1), an exopolyphosphatase (ppx), and a guanosine pentaphosphate phosphohydrolase (gppA).

Within the Root- and Soil-associated *Pantoea* clade, both the phosphorus mobilization repertoire and its genomic organization were conserved. The five strains share the contiguous *pqqABCDEF* operon, the *gcd* locus, the three GADH loci, the C-P lyase cluster with two copies of *phnE* and without *phnO*, the *ugpBAEC* operon next to ugpQ, the two Pst systems, one of them adjacent to the ppx-ppk1 pair, and the region that combines the appA phytase, a copy of *pstS*, and the *phoR-phoB* pair. In all ten clusters, gene order, orientation, and flanking genes are consistent. The Root- and Soil-associated Pantoea clade also carries four members of the PQQ-dependent glucose, quinate, and shikimate dehydrogenase family, of which only the syntenic locus corresponds to Gcd. The only difference in the repertoire was a second copy of *appA*, present in *P. brenneri* 3.1, *Pantoea* sp. 3.5.1, and *P. brenneri* 3.6.1, and absent in *P. brenneri* 3.5.2 and *P. brenneri ZM06*.

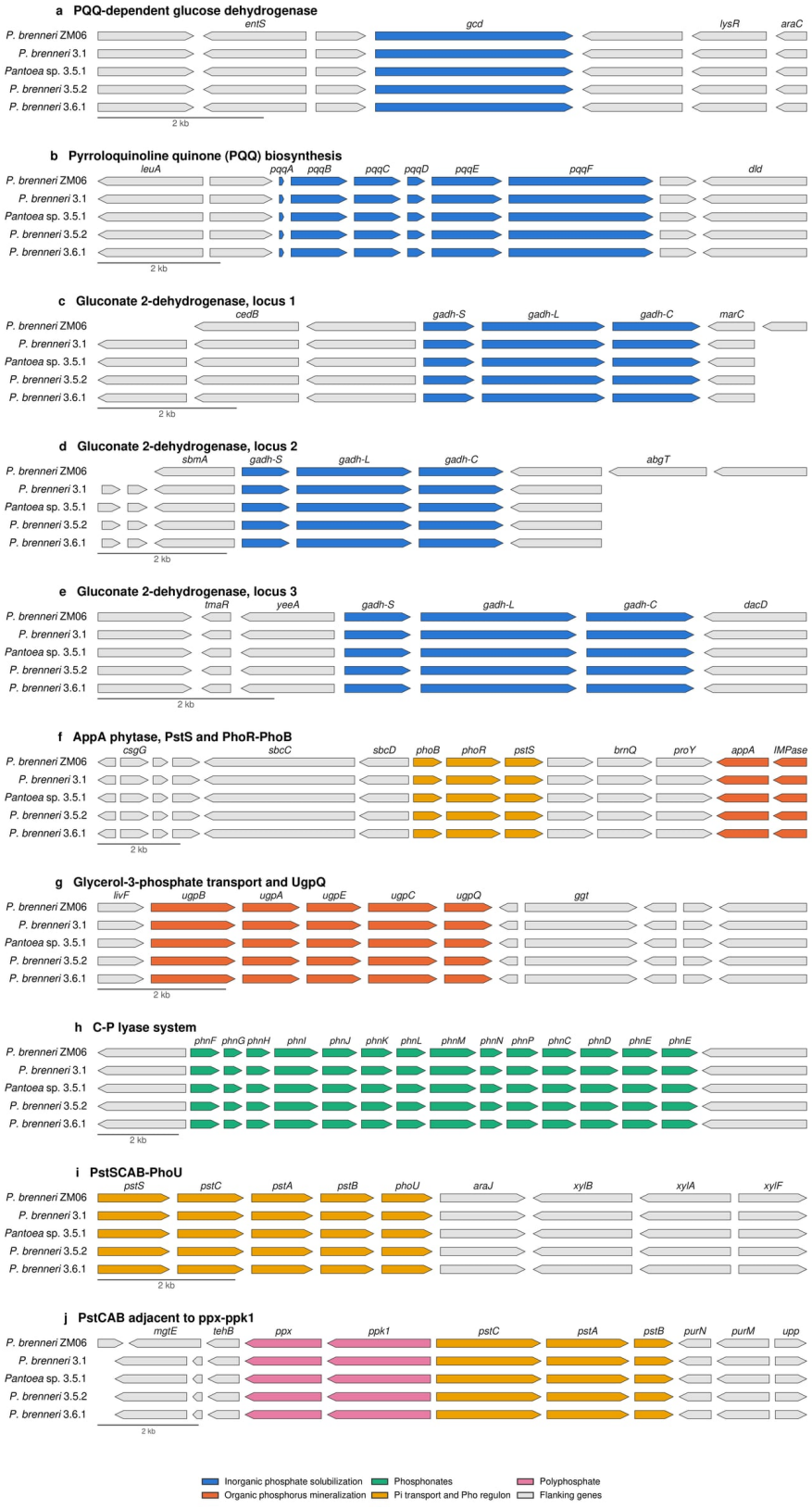


Figure 6. Genomic organization of the gene clusters associated with phosphorus mobilization in the strains of the Root- and Soil-associated *Pantoea* clade. (**a**) Glucose dehydrogenase (*gcd*). (**b**) PQQ biosynthesis operon (*pqqABCDEF*). (**c**–**e**) The three gluconate 2-dehydrogenase loci, with their *gadh-S*, *gadh-L* and *gadh-C* subunits. (**f**) Region combining the *appA* phytase, an inositol monophosphatase, a *pstS* copy and *phoB-phoR*. (**g**) Glycerol-3-phosphate transport system (*ugpBAEC*) and the phosphodiesterase *ugpQ*. (**h**) C-P lyase cluster. (**i**) *pstSCAB-phoU* operon. (**j**) *pstCAB* adjacent to *ppx-ppk1*, without a colocated *pstS*. Arrows represent genes and their direction of transcription.

3.5. Plant Growth-Promoting Determinants

The in-silico search detected 2475 proteins associated with other plant growth-promoting traits (PGPTs) in *Pantoea brenneri* ZM06. These were distributed across the eight top-level categories: plant colonization (840 genes), biofertilization (433), stress control and biocontrol (429), competitive exclusion (334), phytohormone and plant signal production (245), bioremediation (170), stimulation of the plant immune response (16), and putative functions (8) (Table 2).

Table 2. Plant growth-promoting traits (PGPTs) in the Root- and Soil-associated *Pantoea* clade.

Category/Subcategory	*P. brenneri* ZM06	*P. brenneri* 3.1	*Pantoea* sp. 3.5.1	*P. brenneri* 3.5.2	*P. brenneri* 3.6.1
Biofertilization	**433**	**447**	**446**	**409**	**447**
Phosphate solubilization	191	198	197	183	198
Iron acquisition	113	117	117	106	117
Nitrogen acquisition	77	76	76	71	76
Sulfur assimilation/mineralization	36	39	39	33	39
Potassium solubilization	10	10	10	10	10
Carbon dioxide fixation	6	7	7	6	7
Phytohormones and plant signals	**245**	**248**	**248**	**218**	**247**
Plant vitamin production	93	92	92	80	91
Germination stimulation	25	25	25	25	25
Plant signaling volatiles	23	23	23	21	23
Cytokinins/derivative production	21	23	23	17	23
Branching inhibition	20	20	20	20	20
Abscisic acid degradation	17	18	18	16	18
Other terpenoid/derivative production	17	18	18	11	18
Phospholipid production	13	13	13	13	13
Ubiquinone/coenzyme Q production	10	10	10	10	10
Gamma-aminobutyric acid production	5	5	5	4	5
Linolenic acid production	1	1	1	1	1
Plant colonization	**840**	**893**	**893**	**748**	**893**
Plant-derived substrate usage	607	643	643	545	643
Motility/chemotaxis	126	132	132	96	132
Surface attachment	74	82	82	75	82
Root colonization	18	19	19	17	19
Other colonization-related proteins	10	10	10	10	10
Plant cell wall/membrane degradation	3	5	5	3	5
Adaptation to plant immune system	2	2	2	2	2
Competitive exclusion	**334**	**320**	**321**	**279**	**320**
Bacterial fitness	137	139	140	114	139
Cell envelope remodeling	86	87	87	84	87
Quorum-sensing/biofilm formation	60	65	65	55	65
Bacterial secretion	43	20	20	17	20
Exopolysaccharide production/EPS	6	7	7	7	7
Spore production *	2	2	2	2	2
Stress control and biocontrol	**429**	**428**	**427**	**390**	**428**
Neutralizing abiotic stress	305	311	310	287	311
Universal stress response	79	71	71	62	71
Neutralizing biotic stress	45	46	46	41	46
Plant immune stimulation	**16**	**19**	**16**	**16**	**19**
Triggered immunity	16	19	16	16	19

Table 2. *Cont.*

Category/Subcategory	*P. brenneri* ZM06	*P. brenneri* 3.1	*Pantoea* sp. 3.5.1	*P. brenneri* 3.5.2	*P. brenneri* 3.6.1
Bioremediation	**170**	**171**	**171**	**118**	**171**
Heavy metal detoxification	120	112	112	78	112
Xenobiotics biodegradation	46	56	56	38	56
Fluoride detoxification	4	3	3	2	3
Putative functions	8	8	8	7	8
Proteins with a PGPT pathway	**2475**	**2534**	**2530**	**2185**	**2533**

* Assigned by homology to protein families named after *Bacillus subtilis* sporulation proteins, whose conserved members in Enterobacteriaceae and YeaH and YcgB of *Escherichia coli* are not associated with sporulation.

For auxin biosynthesis, the *ipdC* gene was identified, which encodes indole-3-pyruvate decarboxylase, a key enzyme in the conversion of indole-3-pyruvic acid (IPA) to indole-3-acetaldehyde (IAAld). The *aspC* and *tyrB* genes, which encode aminotransferases potentially involved in IPA formation from tryptophan (Trp), were also identified, as well as genes encoding aldehyde dehydrogenases that could participate in the oxidation of IAAld to indole-3-acetic acid (IAA). In contrast, tryptophan 2-monooxygenase (*iaaM*) was not detected, so the indole-3-acetamide (IAM) pathway is likely absent. The genome also encodes genes associated with cytokinin synthesis through tRNA modification (*miaA*, *miaB*, and *miaE*) and the polyamine biosynthesis pathway (*speA-E*). The *acdS* gene, which encodes 1-aminocyclopropane-1-carboxylic acid (ACC) deaminase, was not detected.

Regarding iron acquisition, *P. brenneri ZM06* has the complete enterobactin siderophore biosynthesis cluster (*entA-F*). Uptake systems for exogenous hydroxamate-type siderophores (*fhuBCDF*), ferrous iron (*feoAB*, *efeUOB*), and iron and manganese (*sitABCD*) were also identified. In nitrogen metabolism, the structural nitrogenase genes (*nifHDK*) were not found, but *nifS*, *nifU*, and *nifM* were. The strain therefore has no genetic capacity for biological nitrogen fixation, and these three genes correspond to iron–sulfur cluster assembly functions. The nitrogen-related assignments correspond to assimilation and uptake. In contrast, the genes for respiratory nitrate reductase (*narGHIJ*), assimilatory nitrate reductase (*nasA*), and nitrite reductase (*nirBD*) were detected.

P. brenneri ZM06 also contains the acetoin and 2,3-butanediol synthesis pathway (*budABC*), volatile organic compounds associated with growth promotion and induction of systemic resistance in plants. Finally, genes associated with abiotic stress tolerance were identified, including those for the synthesis and uptake of osmoprotectants such as glycine betaine (*betAB*, *proP*, *opu*) and trehalose (*otsAB*), and potassium uptake systems (*kdpABCDE* and *trk*).

The comparison within the Root- and Soil-associated *Pantoea* clade showed equivalent PGPT profiles, with 2185 to 2534 assigned proteins and a similar density (Table 2). The five strains shared the same number of genes in potassium solubilization (10), germination stimulation (25), branching inhibition (20), phospholipid (13) and ubiquinone (10) production, and adaptation to the plant immune system (2). *P. brenneri* 3.5.2 showed the lowest values in most categories, consistent with its lower number of predicted proteins (3883). The largest differences in *P. brenneri ZM06* corresponded to bacterial secretion (43 genes versus 17 to 20), heavy metal detoxification (120 versus 78 to 112), and universal stress response (79 versus 62 to 71).

3.6. Determinants Associated with Root Colonization

Genome mining in *P. brenneri* ZM06 revealed 840 genes related to plant colonization (Table 2). Most were associated with the use of plant-derived substrates (607 genes), followed by motility and chemotaxis (126), surface attachment (74), root colonization (18), other colonization-related proteins (10), plant cell wall and membrane degradation (3), and adaptation to the plant immune system (2). The motility and chemotaxis set includes two flagellar systems and the chemotaxis system, and the attachment determinants include fimbriae, type IV pili and cellulose biosynthesis.

The genome encodes two complete flagellar systems. The first includes the genes for the basal body and hook (*flg*), the filament and MS ring (*fli*), the motor (*motAB*), the flagellar export system (*flhAB*, *fliHIPQR*), and the master regulators of flagellar transcription (*flhDC*). The second corresponds to the flag-2 system and consists of 29 contiguous genes that include the export system (*flhAB*, *fliRQP*), the MS ring and rotor switch (*fliFGN*), the export ATPase (*fliI*), and the basal body, hook, and filament genes (*flgNMABCDEFGHIKL*). The core chemotaxis components were also identified, namely the sensor histidine kinase (*cheA*), the coupling protein (*cheW*), the methyltransferase (*cheR*), the methylesterase (*cheB*), the response regulator (*cheY*), and the phosphatase that dephosphorylates it (*cheZ*). Likewise, nine genes encoding methyl-accepting chemotaxis proteins (MCPs) were identified, as well as the periplasmic ribose-binding (*rbsB*) and galactose-binding (*mglB*) proteins, which act as attractant receptors. For adhesion, *P. brenneri ZM06* has chaperone–usher pathway fimbriae, with a structural fimbrial protein, two outer membrane usher proteins, and an assembly protein. It also encodes a system homologous to the type IVa pilus, with assembly and membrane proteins (*hofBCMNOPQ*, *ppdABCD*) and assembly and retraction ATPases (*pilB*, *pilT*). Biofilm formation may also be regulated by the two-component systems that respond to envelope stress (*cpxAR*) and acidity (*rstAB*).

P. brenneri ZM06 has a broad repertoire of pathways for the catabolism of compounds present in root exudates and tissues. These include pathways for the degradation of galacturonate (*uxa*), glucuronate (*uxu*), glucarate (*gar*), and galactonate (*dgo*), oligogalacturonides (*kduDI*) and inositol (*iol*), and several β-glucosides. Pathways for the use of phenolic compounds such as gallate, quinate, and protocatechuate, as well as trigonelline (*tgnB*) and putrescine (*puu*), were also identified. RND-family efflux pumps associated with resistance to isothiocyanates and phytoalexins (*acrAB*) were identified, as well as plant compound detoxification enzymes, such as curcumin reductase (*curA*) and the NADPH-dependent quinone reductase (*mdaB*) associated with resistance to 2-methylene-4-butyrolactone.

The repertoire of plant cell wall-degrading enzymes in *P. brenneri ZM06* was limited. A polygalacturonase homolog (GH28 family) was found, as well as β-xylosidase (*xynB*), β-glucosidases, and rhamnogalacturonyl hydrolase (*yteR*). No pectate lyases, pectin methylesterases, xylanases, or extracellular cellulases were detected. In contrast, the genes of the cellulose (*bcsABCZ*) and colanic acid (*wcaKL*) synthesis pathways were identified. Components of a type VI secretion system were detected, distributed across three contigs. The first contains the small subunit of the contractile sheath (*tssB*) and the ImpA protein (*impA*), and the second the tube protein Hcp. The third contains the membrane protein TssM (*tssM*), the IcmH/DotU protein (*icmH*), and the associated proteins TagF (*tagF*) and TagH (*tagH*). No genes of the pathogenicity-associated type III secretion system (*hrp*/*hrc*) were found.

The comparison within the Root- and Soil-associated *Pantoea* clade showed that the strains share the same set of colonization determinants, with the exception of *P. brenneri* 3.5.2. Counts per functional category were equivalent, with 18 root colonization genes in *P. brenneri ZM06* and 17 to 19 in the soil strains, 74 surface adhesion genes in strain ZM06 and 75 to 82 in the soil strains, and 3 plant cell wall and membrane degradation genes in

strain ZM06 and 3 to 5 in the soil strains. *P. brenneri* 3.5.2 was the only strain that departed from the group, as it lacks the second flagellar system, with 43 flagellar genes versus 74 in strain ZM06 and 77 in the other three soil strains, as well as the complete carotenoid cluster present in the others.

4. Discussion

Phosphorus (P) is one of the nutrients that most frequently limit maize yield, because most soil P occurs in forms that roots cannot take up directly [51,52]. Phosphorus-solubilizing and -mineralizing bacteria offer a way to make these reserves available to the crop [52,53]. In Mexico, the Pepitilla maize landrace is grown in Leptosols and marginal soils [54], which are shallow and have low nutrient retention capacity [55], often under traditional low-input systems where plant-available P depends largely on soil biological processes. Our results show that strain ZM06 solubilized phosphate on Pikovskaya medium, with a solubilization index of 2.5 ± 0.11.

The genome provides a mechanism that would account for this phenotype, since it encodes the complete Gcd-PQQ system together with three gluconate 2-dehydrogenase loci and a 2-ketogluconate reductase. Organic acids were not quantified in this work, so the contribution of this route to the observed phenotype remains a prediction derived from gene content. PQQ-dependent glucose dehydrogenase (*gcd*) converts glucose into gluconic acid ($C_6H_{12}O_7$), which is released into the medium, acidifies the surroundings, and chelates the cations that retain phosphate [56]. This mechanism was discovered precisely in this genus. The first mineral phosphate solubilization gene was cloned from *Erwinia herbicola*, now *P. agglomerans* [57], and turned out to be a PQQ biosynthesis gene whose expression was sufficient for *Escherichia coli* HB101, which produces the apoenzyme but not the cofactor, to oxidize glucose to gluconic acid and solubilize phosphate [58]. *P. brenneri ZM06* carries the complete PQQ biosynthesis cluster (*pqqABCDEF*) together with *gcd*, so it can synthesize the cofactor required by the enzyme. The pathway also operates in other members of the genus, as *P. eucalypti* solubilizes phosphate mainly through the secretion and oxidation of gluconic acid [59], and *P. agglomerans* R-42 releases more than 1300 mg L^{-1} of phosphate from calcium phosphates [60].

A second oxidation was also identified in the repertoire of *P. brenneri* ZM06. Its three gluconate 2-dehydrogenase (GADH) loci could convert gluconic acid into 2-ketogluconic acid ($C_6H_{10}O_7$), a stronger acid than its precursor. In *Pseudomonas*, strains of the same species differ in producing gluconic or 2-ketogluconic acid depending on whether they carry the *gad* genes [6]. *P. brenneri ZM06*, in contrast, has this pathway natively and in three copies, so it does not depend on a single locus for this reaction. The substrate for this pathway could be supplied by the plant. Root exudates release sugars, organic acids, and amino acids [61], and a bacterium attached to the rhizoplane, such as *P. brenneri* ZM06, would oxidize that glucose at the same site where the root takes up the released phosphate. However, carrying the pathway does not guarantee its expression. Mutations in *gcd* and *pqqE* markedly reduce solubilization in *Pseudomonas fluorescens* F113 [6], but in *P. brenneri*, inactivation of *gcd* reduced the solubilization index 2.5-fold without abolishing it [62]. In addition, the soil strains of the clade secrete eight organic acids and phosphatases when grown on insoluble phosphates [20]. In *P. brenneri* ZM06, the Gcd-PQQ-GADH system should be understood as the main encoded mechanism and not as the only possible one.

P. brenneri ZM06 also carries two enzymes of the histidine acid phosphatase family, the group to which bacterial phytases belong. The first is a bifunctional glucose-1-phosphatase (*agp*), equivalent to the one characterized in *Pantoea* sp. 3.5.1 of the clade, with high phytase activity and unusual activation by metal ions [63]. The second is a histidine-type phosphatase of the AppA family (*appA*) adjacent to an inositol monophosphatase. This

arrangement is consistent with stepwise dephosphorylation of phytate, although neither the intermediate inositol phosphates nor the final release of inorganic phosphate was measured. Bacteria that combine phytate mineralization with phosphate solubilization are uncommon among rhizosphere isolates [64], and *P. brenneri* ZM06 combines both capacities. Its genome also encodes an alkaline phosphatase (*phoA*), which complements the acid phosphatases above different pH ranges. This combination is relevant because alkaline phosphatase activity decreases in acidic soils [65].

The third pathway corresponds to phosphonates. *P. brenneri* ZM06 retains the 14-gene C-P lyase cluster (*phnCDEFGHIJKLMNP*). The carbon–phosphorus bond resists ordinary hydrolysis, and C-P lyase is the pathway that provides access to this fraction of organic P [66]. Its ecological value has been documented at a large scale, since in 583 soils from Panama and Australia, C-P lyase genes were enriched at sites with the lowest phosphorus availability [67]. The absence of *phnO* does not compromise this pathway in ZM06, since this aminoalkylphosphonate N-acetyltransferase is not required for growth on alkylphosphonates such as methylphosphonate, although it is needed to use 1-aminoalkylphosphonates as a phosphorus source and to detoxify (S)-1-aminoethylphosphonate [68].

Mobilizing phosphate is only useful if the cell captures it before its competitors. Phosphate acquisition requires passage across two barriers. PhoE is an outer membrane porin that lets anions enter the periplasm under phosphate limitation, and PstSCAB is an ABC transporter of the cytoplasmic membrane whose periplasmic binding protein PstS delivers phosphate to the cytoplasm. The assignment of the ZM06 porin to PhoE rests on its genomic context, since the gene lies in the canonical phoE neighbourhood. *P. brenneri* ZM06 has two *pst* loci, in addition to the low-affinity transporter (*pitA*) and *phoE*. The first corresponds to a complete *pstSCAB* operon. The second lacks a colocated *pstS*, so the periplasmic binding protein would have to be supplied in trans by one of the two copies located elsewhere in the genome, and its position next to *ppx* and *ppk1* suggests a link to polyphosphate metabolism rather than a second independent high-affinity transporter. The two-component system (*phoR-phoB*), together with the accessory protein PhoU (*phoU*), couples the external phosphate concentration to the expression of the Pho regulon, one of the most extensive regulatory networks described in bacteria [9]. In P-depleted forest soils, *pstSCAB* genes were more abundant and *phoB-phoR* predominated as a response to limitation [69], a pattern also observed in tropical forest, temperate grassland, and arid shrubland soils [67].

The genetic potential for phosphorus mobilization is therefore conserved among the five strains examined and does not segregate with the isolation source, in contrast with *Pseudomonas*, where strains of the same species differ in the gluconate oxidation pathway [6]. The only difference corresponds to a second copy of *appA*, present in *P. brenneri* 3.1, *Pantoea* sp. 3.5.1, and *P. brenneri* 3.6.1, and absent in *P. brenneri* ZM06 and *P. brenneri* 3.5.2. This difference has a biochemical correlate, because *P. brenneri* 3.5.2 lacks the esterase-type phytase activity present in the other strains [21]. This leads to a testable prediction, namely that *P. brenneri* ZM06 shares the phytase profile of *P. brenneri* 3.5.2, with an activity dependent on Agp and a single AppA. What varies within the clade is, therefore, the hydrolysis of phytate, the most recalcitrant fraction of organic P.

We had expected genomic variation to involve the determinants associated with root colonization. This was not the case: *P. brenneri* ZM06 retains the complete colonization repertoire, from chemotaxis and flagellar motility to fimbriae, type IV pili and cellulose, but the soil strains carry the same repertoire, except *P. brenneri* 3.5.2, which lacks the second flagellar system and the carotenoid cluster. Loss of motility or chemotaxis reduces colonization efficiency up to 100-fold [70], and in the Root- and Soil-associated *Pantoea* clade these systems are conserved. Functional evidence points in the same direction, as *Pantoea*

sp. 3.5.1 and *P. brenneri* 3.5.2 colonize wheat roots and leaves, with up to 2.5×10^{11} CFU per gram of root [71]. The isolation of *P. brenneri* ZM06 from the rhizoplane may reflect the order of arrival at the root rather than a distinct gene content, since in *P. agglomerans* early colonizers have an advantage over late ones [72].

The rest of the profile of *P. brenneri* ZM06 is complemented by indole-3-acetic acid synthesis via the indole-3-pyruvate pathway (*ipdC*) [73], iron uptake via enterobactin [74], and acetoin and 2,3-butanediol synthesis (*budABC*), volatile compounds that promote growth [75]. In contrast, *P. brenneri* ZM06 lacks nitrogenase and ACC deaminase (*acdS*), two functions that within the genus are restricted to particular lineages [16,76].

5. Integrated Model of Phosphorus Mobilization and Homeostasis

Based on the genomic data, the pathways of *P. brenneri* ZM06 may not operate in isolation but rather may be integrated into a system that couples root colonization with phosphorus acquisition (Figure 7). The rhizoplane supplies the carbon that fuels the gluconic acid pathway. Gcd oxidizes glucose from root exudates in the periplasm, and the released gluconic and 2-ketogluconic acids dissolve calcium phosphates and can chelate iron and aluminum. Solubilization is thus coupled to colonization, because without adhesion to the root surface and access to exudates, the pathway lacks substrate. Colonization depends on chemotaxis and flagellar motility, whose loss reduces its efficiency up to 100-fold [70], and *P. brenneri* ZM06 retains two flagellar systems, the chemotaxis system and the adhesion determinants.

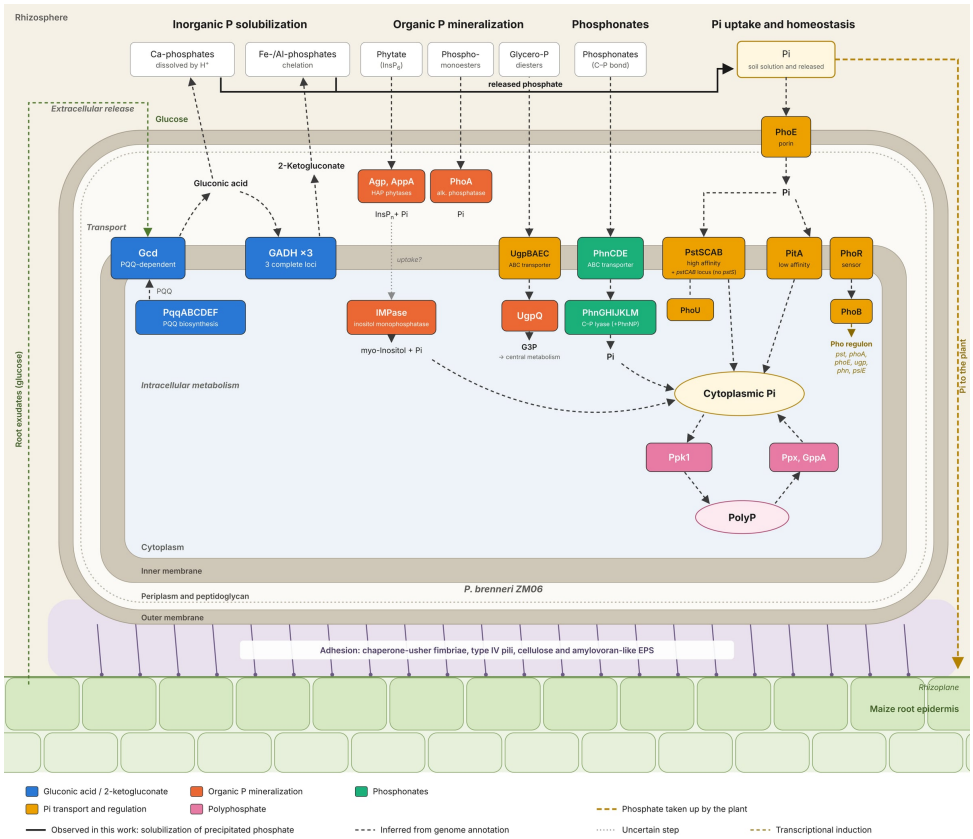


Figure 7. Model of phosphorus mobilization and homeostasis in *P. brenneri* ZM06 at the maize rhizoplane, inferred from its genome. The pathways are grouped by compartment: extracellular release of phosphate, uptake across the outer and cytoplasmic membranes, and intracellular metabolism and storage. Solid arrows indicate the step verified experimentally in this work. Dashed arrows indicate steps predicted from gene content, including the transfer of phosphate to the plant.

The mobilization pathways act on distinct, nonredundant pools and in different compartments, and they do not contribute equally to the phosphorus available to the plant. Acidolysis is the only step that operates in the soil solution, where gluconic and 2-ketogluconic acids release calcium-bound phosphate. The phytases Agp and AppA hydrolyze phytate, which can represent up to 45% of soil organic phosphorus and remains at very low concentrations in solution because of its strong adsorption to oxides [77], and PhoA releases phosphate from phosphomonoesters. Both are predicted to be periplasmic, so the phosphate they release is liberated within the cell envelope and is largely retained. Phosphate from the soil solution enters through PhoE, the two Pst systems and PitA, whereas glycerophosphodiesters and phosphonates are used inside the cell through the Ugp system and C-P lyase, which support bacterial nutrition without releasing phosphate to the rhizosphere. The Pho regulon, activated by PhoR-PhoB when dissolved phosphate is scarce, coordinates the induction of *pst*, *phoA*, *ugp*, and *phn*, and the proximity of a *pstS* copy and *phoR-phoB* to the *appA* phytase suggests that phytate mineralization would also be part of this response.

Polyphosphate adds a temporal dimension, because root exudation and phosphate release occur in pulses. Ppk1 synthesizes polyphosphate from ATP and Ppx hydrolyzes it, so storage when phosphate is abundant and mobilization when it becomes scarce would allow the cell to buffer variation in supply. GppA is also encoded, but its characterized activity is the conversion of guanosine pentaphosphate (pppGpp) to guanosine tetraphosphate (ppGpp), although the *E. coli* enzyme also hydrolyzes long-chain polyphosphate in vitro [78], and substrate preference within the PPX/GPPA family cannot be inferred from sequence similarity, so its participation in polyphosphate turnover remains a prediction.

Overall, the presence of these pathways is consistent with a bacterium adapted to phosphorus-limited soils, such as the Leptosols and marginal soils where the "Pepitilla" landrace maize is grown [54]. Whether colonization by this strain produces a net increase in the phosphorus available to maize depends on the balance between release and uptake, which was not determined in this work.

6. Limitations and Future Directions

The pathways described here were identified from genome sequences, so they define genetic potential rather than demonstrated activity: gene expression was not measured, and no inoculation or colonization experiment was performed with *P. brenneri* ZM06. Because the species was described from human clinical isolates, the assembly was screened for resistance and virulence determinants, and no acquired resistance genes, toxins or type III secretion system determinants were detected, although a sequence-based screen does not replace the phenotypic assessment required before any field application.

Gene presence is therefore not a sufficient criterion for strain selection, as shown in *Pantoea rara*, where mutants with contrasting solubilization indices were indistinguishable in their canonical genes [79]. What remains to be established for *P. brenneri* ZM06 is quantitative: the solubilization of phosphate in liquid culture; the identity and amount of the organic acids released, by high-performance liquid chromatography and, for acids other than gluconate and 2-ketogluconate, by untargeted metabolomics; the activity of its phytases; and the expression of these pathways under phosphate limitation by RNA sequencing. Long-read sequencing would close the assembly and resolve copy number and cluster boundaries.

Whether the strain works as a bioinoculant requires a stepwise evaluation under phosphorus limitation. In the greenhouse, the phosphorus content and the biomass of inoculated maize would be compared with uninoculated controls and with phosphate fertilization, in the Leptosols and marginal soils where the Pepitilla landrace is grown [54]. In the field, the survival of the strain, its colonization of the root over the crop cycle and

the effect of both on yield would determine its agronomic value. Inoculation of maize with solubilizing bacteria has improved growth and yield in P-deficient soils [12–14], including with bacteria from Mexican maize and its wild relatives [80–82], so the question for *P. brenneri* ZM06 is whether the pathways described here translate into measurable phosphorus uptake by the plant.

Supplementary Materials: The following supporting information can be downloaded at https://www.mdpi.com/article/10.3390/microorganisms14122753/s1: Table S1: *P. brenneri* ZM06 and the 36 RefSeq reference genomes used in the comparative analyses, with their genomic characteristics. Table S2: Curated database of reference proteins obtained from UniProt and used to verify the functional assignment of the phosphorus mobilization and homeostasis genes. Table S3: Locus tags, contigs, coordinates and annotations of the phosphorus mobilization and homeostasis genes in *P. brenneri* ZM06. Table S4: Average nucleotide identity (ANI) matrix of *P. brenneri* ZM06 and the 36 *Pantoea* reference genomes. Table S5: Average amino acid identity (AAI) matrix of *P. brenneri* ZM06 and the 36 *Pantoea* reference genomes. Table S6: Digital DNA-DNA hybridization (dDDH) values between *P. brenneri* ZM06 and its four closest relatives from soil. Table S7: The 211 orthologous groups exclusive to *P. brenneri* ZM06, with their locus tags, annotations, genomic coordinates and eggNOG functional assignments.

Author Contributions: Conceptualization, J.L.A.-N. and G.C.-F.; methodology, J.L.A.-N. and G.C.-F.; software, J.L.A.-N. and G.C.-F.; formal analysis, G.C.-F. and L.J.G.-G.; investigation, G.C.-F., L.J.G.-G. and J.L.A.-N.; resources, J.L.A.-N.; data curation, M.A.R.-M., J.D.C.-Z. and A.A.-M.; writing—original draft preparation, J.L.A.-N.; writing—review and editing, J.L.A.-N., G.C.-F., M.A.R.-M., J.D.C.-Z. and A.A.-M.; funding acquisition, J.L.A.-N. All authors have read and agreed to the published version of the manuscript.

Funding: This work was funded by Secretaría de Ciencia, Humanidades, Tecnología e Innovación (SECIHTI) (PEE-2025-G-248).

Institutional Review Board Statement: Not applicable.

Informed Consent Statement: Not applicable.

Data Availability Statement: The genome assembly of *P. brenneri* ZM06 is available in GenBank under accession GCA_062061765.1 (BioSample SAMN64265162). The raw sequencing reads were deposited in the Sequence Read Archive (SRA) under accession number SRR41786847. Both are part of BioProject PRJNA1545390 (https://www.ncbi.nlm.nih.gov/bioproject/PRJNA1545390; accessed on 24 November 2026).

Acknowledgments: We thank UATI for their expert technical support and server maintenance at Centro de Ciencias Genómicas, UNAM.

Conflicts of Interest: The authors declare no conflicts of interest.

References

1. Pang, F.; Li, Q.; Solanki, M.K.; Wang, Z.; Xing, Y.-X.; Dong, D.-F. Soil Phosphorus Transformation and Plant Uptake Driven by Phosphate-Solubilizing Microorganisms. *Front. Microbiol.* **2024**, *15*, 1383813. [CrossRef] [PubMed]
2. Sun, X.; Tian, X.; Jia, M.; Hu, X.; Zhang, C.; Zhao, L. Phosphate-Solubilizing Bacteria: A Review of Diversity, Mechanisms, and Applications in Sustainable Agriculture. *Front. Microbiol.* **2026**, *17*, 1778470. [CrossRef] [PubMed]
3. Gérard, F. Clay Minerals, Iron/Aluminum Oxides, and Their Contribution to Phosphate Sorption in Soils. A Myth Revisited. *Geoderma* **2016**, *262*, 213–226. [CrossRef]
4. Tunesi, S.; Poggi, V.; Gessa, C. Phosphate Adsorption and Precipitation in Calcareous Soils: The Role of Calcium Ions in Solution and Carbonate Minerals. *Nutr. Cycl. Agroecosyst.* **1999**, *53*, 219–227. [CrossRef]
5. Ughamba, K.T.; Ndukwe, J.K.; Lidbury, I.D.E.A.; Nnaji, N.D.; Eze, C.N.; Aduba, C.C.; Groenhof, S.; Chukwu, K.O.; Anyanwu, C.U.; Nwaiwu, O.; et al. Trends in the Application of Phosphate-Solubilizing Microbes as Biofertilizers: Implications for Soil Improvement. *Soil Syst.* **2025**, *9*, 6. [CrossRef]

6. Miller, S.H.; Browne, P.; Prigent-Combaret, C.; Combes-Meynet, E.; Morrissey, J.P.; O'Gara, F. Biochemical and Genomic Comparison of Inorganic Phosphate Solubilization in *Pseudomonas* Species. *Environ. Microbiol. Rep.* **2010**, *2*, 403–411. [CrossRef] [PubMed]
7. Wang, J.; Yu, X.; Dong, P.; Li, Y.; Zhang, Y.; Wang, G. Mechanisms and Research Progress of Phosphate-Solubilizing Microorganisms in Promoting Sustainable Crop Production. *Microorganisms* **2026**, *14*, 2022. [CrossRef] [PubMed]
8. Kim, K.Y.; Hwangbo, H.; Park, R.D.; Kim, Y.W.; Rim, Y.S.; Park, K.H.; Kim, T.H.; Suh, J.S. 2-Ketogluconic Acid Production and Phosphate Solubilization by *Enterobacter intermedium*. *Curr. Microbiol.* **2003**, *47*, 87–92. [CrossRef] [PubMed]
9. Santos-Beneit, F. The Pho Regulon: A Huge Regulatory Network in Bacteria. *Front. Microbiol.* **2015**, *6*, 402. [CrossRef] [PubMed]
10. Srivastava, S.; Anand, V.; Kaur, J.; Ranjan, M.; Bist, V.; Asif, M.H.; Srivastava, S. Functional Genetic Diversity and Plant Growth Promoting Potential of Polyphosphate Accumulating Bacteria in Soil. *Microbiol. Spectr.* **2022**, *10*, e00345-21. [CrossRef] [PubMed]
11. Neville, N.; Roberge, N.; Jia, Z. Polyphosphate Kinase 2 (PPK2) Enzymes: Structure, Function, and Roles in Bacterial Physiology and Virulence. *Int. J. Mol. Sci.* **2022**, *23*, 670. [CrossRef] [PubMed]
12. Pereira, S.I.A.; Castro, P.M.L. Phosphate-Solubilizing Rhizobacteria Enhance *Zea mays* Growth in Agricultural P-Deficient Soils. *Ecol. Eng.* **2014**, *73*, 526–535. [CrossRef]
13. Viruel, E.; Erazzú, L.E.; Martínez Calsina, L.; Ferrero, M.A.; Lucca, M.E.; Siñeriz, F. Inoculation of Maize with Phosphate Solubilizing Bacteria: Effect on Plant Growth and Yield. *J. Soil Sci. Plant Nutr.* **2014**, *14*, 819–831. [CrossRef]
14. de Oliveira-Paiva, C.A.; Bini, D.; de Sousa, S.M.; Ribeiro, V.P.; dos Santos, F.C.; de Paula Lana, U.G.; de Souza, F.F.; Gomes, E.A.; Marriel, I.E. Inoculation with *Bacillus megaterium* CNPMS B119 and *Bacillus subtilis* CNPMS B2084 Improve P-Acquisition and Maize Yield in Brazil. *Front. Microbiol.* **2024**, *15*, 1426166. Erratum in *Front. Microbiol.* **2026**, *17*, 1850844.. [CrossRef] [PubMed]
15. Chen, X.; Zhao, Y.; Huang, S.; Peñuelas, J.; Sardans, J.; Wang, L.; Zheng, B. Genome-Based Identification of Phosphate-Solubilizing Capacities of Soil Bacterial Isolates. *AMB Express* **2024**, *14*, 85. [CrossRef] [PubMed]
16. Rimes-Casais, F.F.; Pedrosa-Silva, F.; Venancio, T.M. Comparative Genomic Insights into the Genus *Pantoea*: Genetic Determinants of Ecological Lifestyle Diversity and Plant Growth-Promoting Potential. *World J. Microbiol. Biotechnol.* **2026**, *42*, 46. [CrossRef] [PubMed]
17. Yang, F.; Li, M.; Wu, H.; Yu, C.; Liu, W.; Chen, H. Comparative Genomics-Based Insights into *Pantoea ananatis* Strains, Isolated from White Spot Diseased Leaves of Maize with Plant Growth-Promoting Attributes. *Appl. Environ. Microbiol.* **2025**, *91*, e00329-25. [CrossRef] [PubMed]
18. Duchateau, S.; Crouzet, J.; Dorey, S.; Aziz, A. The Plant-Associated *Pantoea* spp. as Biocontrol Agents: Mechanisms and Diversity of Bacteria-Produced Metabolites as a Prospective Tool for Plant Protection. *Biol. Control* **2024**, *188*, 105441. [CrossRef]
19. Brady, C.L.; Cleenwerck, I.; Venter, S.N.; Engelbeen, K.; De Vos, P.; Coutinho, T.A. Emended Description of the Genus *Pantoea*, Description of Four Species from Human Clinical Samples, *Pantoea septica* sp. nov., *Pantoea eucrina* sp. nov., *Pantoea brenneri* sp. nov. and *Pantoea conspicua* sp. nov. *Int. J. Syst. Evol. Microbiol.* **2010**, *60*, 2430–2440. [CrossRef] [PubMed]
20. Suleimanova, A.; Bulmakova, D.; Sokolnikova, L.; Egorova, E.; Itkina, D.; Kuzminova, O.; Gizatullina, A.; Sharipova, M. Phosphate Solubilization and Plant Growth Promotion by *Pantoea brenneri* Soil Isolates. *Microorganisms* **2023**, *11*, 1136. [CrossRef] [PubMed]
21. Suleimanova, A.; Pudova, D.; Sokolnikova, L.; Shagimardanova, E.; Sharipova, M. Genome Sequence Data of Phytase-Producing Strains of *Pantoea brenneri*. *Microbiol. Resour. Announc.* **2025**, *14*, e01032-25. [CrossRef] [PubMed]
22. Herrera-Quiterio, A.; Toledo-Hernández, E.; Aguirre-Noyola, J.L.; Romero, Y.; Ramos, J.; Palemón-Alberto, F.; Toribio-Jiménez, J. Antagonic and Plant Growth-Promoting Effects of Bacteria Isolated from Mine Tailings at El Fraile, Mexico. *Rev. Argent. Microbiol.* **2020**, *52*, 231–239. [CrossRef] [PubMed]
23. Andrews, S. FastQC: A Quality Control Tool for High Throughput Sequence Data. Available online: https://www.bioinformatics.babraham.ac.uk/projects/fastqc/ (accessed on 15 November 2026).
24. Krueger, F. *Trim Galore, Version 0.6.10*; Zenodo: Geneva, Switzerland, 2023. [CrossRef]
25. Wick, R.R.; Judd, L.M.; Gorrie, C.L.; Holt, K.E. Unicycler: Resolving Bacterial Genome Assemblies from Short and Long Sequencing Reads. *PLoS Comput. Biol.* **2017**, *13*, e1005595. [CrossRef] [PubMed]
26. Parks, D.H.; Imelfort, M.; Skennerton, C.T.; Hugenholtz, P.; Tyson, G.W. CheckM: Assessing the Quality of Microbial Genomes Recovered from Isolates, Single Cells, and Metagenomes. *Genome Res.* **2015**, *25*, 1043–1055. [CrossRef] [PubMed]
27. Bushnell, B. BBMap: A Fast, Accurate, Splice-Aware Aligner. Available online: https://bbmap.org (accessed on 15 November 2026).
28. Schwengers, O.; Jelonek, L.; Dieckmann, M.A.; Beyvers, S.; Blom, J.; Goesmann, A. Bakta: Rapid and Standardized Annotation of Bacterial Genomes via Alignment-Free Sequence Identification. *Microb. Genom.* **2021**, *7*, 000685. [CrossRef] [PubMed]
29. Seemann, T. ABRicate: Mass Screening of Contigs for Antimicrobial and Virulence Genes. Available online: https://github.com/tseemann/abricate (accessed on 15 November 2026).
30. Chaumeil, P.A.; Mussig, A.J.; Hugenholtz, P.; Parks, D.H. GTDB-Tk v2: Memory Friendly Classification with the Genome Taxonomy Database. *Bioinformatics* **2022**, *38*, 5315–5316. [CrossRef] [PubMed]

31. Pritchard, L.; Glover, R.H.; Humphris, S.; Elphinstone, J.G.; Toth, I.K. Genomics and Taxonomy in Diagnostics for Food Security: Soft-Rotting Enterobacterial Plant Pathogens. *Anal. Methods* **2016**, *8*, 12–24. [CrossRef]
32. Meier-Kolthoff, J.P.; Auch, A.F.; Klenk, H.P.; Göker, M. Genome Sequence-Based Species Delimitation with Confidence Intervals and Improved Distance Functions. *BMC Bioinform.* **2013**, *14*, 60. [CrossRef] [PubMed]
33. Meier-Kolthoff, J.P.; Göker, M. TYGS Is an Automated High-Throughput Platform for State-of-the-Art Genome-Based Taxonomy. *Nat. Commun.* **2019**, *10*, 2182. [CrossRef] [PubMed]
34. Contreras-Moreira, B.; Vinuesa, P. GET_HOMOLOGUES, a Versatile Software Package for Scalable and Robust Microbial Pangenome Analysis. *Appl. Environ. Microbiol.* **2013**, *79*, 7696–7701. [CrossRef] [PubMed]
35. Vinuesa, P.; Ochoa-Sánchez, L.E.; Contreras-Moreira, B. GET_PHYLOMARKERS, a Software Package to Select Optimal Orthologous Clusters for Phylogenomics and Inferring Pan-Genome Phylogenies, Used for a Critical Geno-Taxonomic Revision of the Genus *Stenotrophomonas*. *Front. Microbiol.* **2018**, *9*, 771. [CrossRef] [PubMed]
36. Cantalapiedra, C.P.; Hernández-Plaza, A.; Letunic, I.; Bork, P.; Huerta-Cepas, J. eggNOG-Mapper v2: Functional Annotation, Orthology Assignments, and Domain Prediction at the Metagenomic Scale. *Mol. Biol. Evol.* **2021**, *38*, 5825–5829. [CrossRef] [PubMed]
37. Huerta-Cepas, J.; Szklarczyk, D.; Heller, D.; Hernández-Plaza, A.; Forslund, S.K.; Cook, H.; Mende, D.R.; Letunic, I.; Rattei, T.; Jensen, L.J.; et al. eggNOG 5.0: A Hierarchical, Functionally and Phylogenetically Annotated Orthology Resource Based on 5090 Organisms and 2502 Viruses. *Nucleic Acids Res.* **2019**, *47*, D309–D314. [CrossRef] [PubMed]
38. Minh, B.Q.; Schmidt, H.A.; Chernomor, O.; Schrempf, D.; Woodhams, M.D.; von Haeseler, A.; Lanfear, R. IQ-TREE 2: New Models and Efficient Methods for Phylogenetic Inference in the Genomic Era. *Mol. Biol. Evol.* **2020**, *37*, 1530–1534. Erratum in *Mol. Biol. Evol.* **2020**, *37*, 2461. [CrossRef] [PubMed]
39. Kalyaanamoorthy, S.; Minh, B.Q.; Wong, T.K.F.; von Haeseler, A.; Jermiin, L.S. ModelFinder: Fast Model Selection for Accurate Phylogenetic Estimates. *Nat. Methods* **2017**, *14*, 587–589. [CrossRef] [PubMed]
40. Guindon, S.; Dufayard, J.F.; Lefort, V.; Anisimova, M.; Hordijk, W.; Gascuel, O. New Algorithms and Methods to Estimate Maximum-Likelihood Phylogenies: Assessing the Performance of PhyML 3.0. *Syst. Biol.* **2010**, *59*, 307–321. [CrossRef] [PubMed]
41. Anisimova, M.; Gil, M.; Dufayard, J.F.; Dessimoz, C.; Gascuel, O. Survey of Branch Support Methods Demonstrates Accuracy, Power, and Robustness of Fast Likelihood-Based Approximation Schemes. *Syst. Biol.* **2011**, *60*, 685–699. [CrossRef] [PubMed]
42. Hoang, D.T.; Chernomor, O.; von Haeseler, A.; Minh, B.Q.; Vinh, L.S. UFBoot2: Improving the Ultrafast Bootstrap Approximation. *Mol. Biol. Evol.* **2018**, *35*, 518–522. [CrossRef] [PubMed]
43. Hyatt, D.; Chen, G.L.; LoCascio, P.F.; Land, M.L.; Larimer, F.W.; Hauser, L.J. Prodigal: Prokaryotic Gene Recognition and Translation Initiation Site Identification. *BMC Bioinform.* **2010**, *11*, 119. [CrossRef] [PubMed]
44. Patz, S.; Gautam, A.; Becker, M.; Ruppel, S.; Rodríguez-Palenzuela, P.; Huson, D.H. PLaBAse: A Comprehensive Web Resource for Analyzing the Plant Growth-Promoting Potential of Plant-Associated Bacteria. *bioRxiv* **2021**. [CrossRef]
45. Pellegrinetti, T.A.; Monteiro, G.G.T.N.; Lemos, L.N.; Santos, R.A.C.; Barros, A.G.; Mendes, L.W. PGPg_finder: A Comprehensive and User-Friendly Pipeline for Identifying Plant Growth-Promoting Genes in Genomic and Metagenomic Data. *Rhizosphere* **2024**, *30*, 100905. [CrossRef]
46. Buchfink, B.; Reuter, K.; Drost, H.G. Sensitive Protein Alignments at Tree-of-Life Scale Using DIAMOND. *Nat. Methods* **2021**, *18*, 366–368. [CrossRef] [PubMed]
47. Martínez-García, P.M.; López-Solanilla, E.; Ramos, C.; Rodríguez-Palenzuela, P. Prediction of Bacterial Associations with Plants Using a Supervised Machine-Learning Approach. *Environ. Microbiol.* **2016**, *18*, 4847–4861. [CrossRef] [PubMed]
48. Camacho, C.; Coulouris, G.; Avagyan, V.; Ma, N.; Papadopoulos, J.; Bealer, K.; Madden, T.L. BLAST+: Architecture and Applications. *BMC Bioinform.* **2009**, *10*, 421. [CrossRef] [PubMed]
49. Gilchrist, C.L.M.; Chooi, Y.H. clinker & clustermap.js: Automatic Generation of Gene Cluster Comparison Figures. *Bioinformatics* **2021**, *37*, 2473–2475. [CrossRef] [PubMed]
50. Navarro-Muñoz, J.C.; Selem-Mojica, N.; Mullowney, M.W.; Kautsar, S.A.; Tryon, J.H.; Parkinson, E.I.; De Los Santos, E.L.C.; Yeong, M.; Cruz-Morales, P.; Abubucker, S.; et al. A Computational Framework to Explore Large-Scale Biosynthetic Diversity. *Nat. Chem. Biol.* **2020**, *16*, 60–68. [CrossRef] [PubMed]
51. Vance, C.P.; Uhde-Stone, C.; Allan, D.L. Phosphorus Acquisition and Use: Critical Adaptations by Plants for Securing a Nonrenewable Resource. *New Phytol.* **2003**, *157*, 423–447. [CrossRef] [PubMed]
52. Richardson, A.E.; Simpson, R.J. Soil Microorganisms Mediating Phosphorus Availability. *Plant Physiol.* **2011**, *156*, 989–996. [CrossRef] [PubMed]
53. Rodríguez, H.; Fraga, R. Phosphate Solubilizing Bacteria and Their Role in Plant Growth Promotion. *Biotechnol. Adv.* **1999**, *17*, 319–339. [CrossRef] [PubMed]
54. Gómez-Montiel, N.O.; Cantú-Almaguer, M.A.; Hernández-Galeno, C.A.; Vázquez-Carrillo, M.G.; Aragón-Cuevas, F.; Espinosa-Calderón, A.; Palemón-Alberto, F. V-236 P, Cultivar de Maíz Pepitilla para Regiones de Montaña Baja. *Rev. Mex. Cienc. Agríc.* **2014**, *5*, 1309–1313. [CrossRef]

55. IUSS Working Group WRB. *World Reference Base for Soil Resources: International Soil Classification System for Naming Soils and Creating Legends for Soil Maps*, 4th ed.; International Union of Soil Sciences (IUSS): Vienna, Austria, 2022.
56. Sashidhar, B.; Podile, A.R. Mineral Phosphate Solubilization by Rhizosphere Bacteria and Scope for Manipulation of the Direct Oxidation Pathway Involving Glucose Dehydrogenase. *J. Appl. Microbiol.* **2010**, *109*, 1–12. [CrossRef] [PubMed]
57. Goldstein, A.H.; Liu, S.T. Molecular Cloning and Regulation of a Mineral Phosphate Solubilizing Gene from *Erwinia herbicola*. *Nat. Biotechnol.* **1987**, *5*, 72–74. [CrossRef]
58. Liu, S.T.; Lee, L.Y.; Tai, C.Y.; Hung, C.H.; Chang, Y.S.; Wolfram, J.H.; Rogers, R.; Goldstein, A.H. Cloning of an *Erwinia herbicola* Gene Necessary for Gluconic Acid Production and Enhanced Mineral Phosphate Solubilization in *Escherichia coli* HB101: Nucleotide Sequence and Probable Involvement in Biosynthesis of the Coenzyme Pyrroloquinoline Quinone. *J. Bacteriol.* **1992**, *174*, 5814–5819. [CrossRef] [PubMed]
59. Castagno, L.N.; Estrella, M.J.; Sannazzaro, A.I.; Grassano, A.E.; Ruiz, O.A. Phosphate-Solubilization Mechanism and *In Vitro* Plant Growth Promotion Activity Mediated by *Pantoea eucalypti* Isolated from *Lotus tenuis* Rhizosphere in the Salado River Basin (Argentina). *J. Appl. Microbiol.* **2011**, *110*, 1151–1165. [CrossRef] [PubMed]
60. Son, H.J.; Park, G.T.; Cha, M.S.; Heo, M.S. Solubilization of Insoluble Inorganic Phosphates by a Novel Salt- and pH-Tolerant *Pantoea agglomerans* R-42 Isolated from Soybean Rhizosphere. *Bioresour. Technol.* **2006**, *97*, 204–210. [CrossRef] [PubMed]
61. Badri, D.V.; Vivanco, J.M. Regulation and Function of Root Exudates. *Plant Cell Environ.* **2009**, *32*, 666–681. [CrossRef]
62. Suleimanova, A.D.; Sokolnikova, L.V.; Bulmakova, D.S.; Egorova, E.A.; Sharipova, M.R. Inactivation of the Gene Responsible for the Synthesis of Gluconic Acid in the Genome of *Pantoea brenneri*. *Microbiology* **2025**, *94*, 286–289. [CrossRef]
63. Suleimanova, A.D.; Beinhauer, A.; Valeeva, L.R.; Chastukhina, I.B.; Balaban, N.P.; Shakirov, E.V.; Greiner, R.; Sharipova, M.R. Novel Glucose-1-Phosphatase with High Phytase Activity and Unusual Metal Ion Activation from Soil Bacterium *Pantoea* sp. Strain 3.5.1. *Appl. Environ. Microbiol.* **2015**, *81*, 6790–6799. [CrossRef] [PubMed]
64. Jorquera, M.A.; Hernández, M.T.; Rengel, Z.; Marschner, P.; Mora, M.L. Isolation of Culturable Phosphobacteria with Both Phytate-Mineralization and Phosphate-Solubilization Activity from the Rhizosphere of Plants Grown in a Volcanic Soil. *Biol. Fertil. Soils* **2008**, *44*, 1025–1034. [CrossRef]
65. Lidbury, I.D.E.A.; Fraser, T.; Murphy, A.R.J.; Scanlan, D.J.; Bending, G.D.; Jones, A.M.E.; Moore, J.D.; Goodall, A.; Tibbett, M.; Hammond, J.P.; et al. The 'Known' Genetic Potential for Microbial Communities to Degrade Organic Phosphorus Is Reduced in Low-pH Soils. *MicrobiologyOpen* **2017**, *6*, e00474. [CrossRef] [PubMed]
66. Villarreal-Chiu, J.F.; Quinn, J.P.; McGrath, J.W. The Genes and Enzymes of Phosphonate Metabolism by Bacteria, and Their Distribution in the Marine Environment. *Front. Microbiol.* **2012**, *3*, 19. [CrossRef] [PubMed]
67. Oliverio, A.M.; Bissett, A.; McGuire, K.; Saltonstall, K.; Turner, B.L.; Fierer, N. The Role of Phosphorus Limitation in Shaping Soil Bacterial Communities and Their Metabolic Capabilities. *mBio* **2020**, *11*, e01718-20. [CrossRef] [PubMed]
68. Hove-Jensen, B.; McSorley, F.R.; Zechel, D.L. Catabolism and Detoxification of 1-Aminoalkylphosphonic Acids: N-Acetylation by the *phnO* Gene Product. *PLoS ONE* **2012**, *7*, e46416. [CrossRef] [PubMed]
69. Bergkemper, F.; Schöler, A.; Engel, M.; Lang, F.; Krüger, J.; Schloter, M.; Schulz, S. Phosphorus Depletion in Forest Soils Shapes Bacterial Communities Towards Phosphorus Recycling Systems. *Environ. Microbiol.* **2016**, *18*, 1988–2000. Erratum in *Environ. Microbiol.* **2016**, *18*, 2767. [CrossRef] [PubMed]
70. Liu, Y.; Xu, Z.; Chen, L.; Xun, W.; Shu, X.; Chen, Y.; Sun, X.; Wang, Z.; Ren, Y.; Shen, Q.; et al. Root Colonization by Beneficial Rhizobacteria. *FEMS Microbiol. Rev.* **2024**, *48*, fuad066. [CrossRef] [PubMed]
71. Sokolnikova, L.V.; Suleimanova, A.D.; Islamov, R.R.; Vasilyeva, E.S.; Sharipova, M.R. The Ability of *Pantoea brenneri* Strains 3.5.1 and 3.5.2 to Colonize Wheat Plants. *Microbiology* **2026**, *95*, 426–428. [CrossRef]
72. Soluch, R.; Hülter, N.F.; Romero Picazo, D.; Özkurt, E.; Stukenbrock, E.H.; Dagan, T. Colonization Dynamics of *Pantoea agglomerans* in the Wheat Root Habitat. *Environ. Microbiol.* **2021**, *23*, 2260–2273. [CrossRef] [PubMed]
73. Spaepen, S.; Vanderleyden, J.; Remans, R. Indole-3-Acetic Acid in Microbial and Microorganism-Plant Signaling. *FEMS Microbiol. Rev.* **2007**, *31*, 425–448. [CrossRef] [PubMed]
74. Raymond, K.N.; Dertz, E.A.; Kim, S.S. Enterobactin: An Archetype for Microbial Iron Transport. *Proc. Natl. Acad. Sci. USA* **2003**, *100*, 3584–3588. [CrossRef] [PubMed]
75. Ryu, C.M.; Farag, M.A.; Hu, C.H.; Reddy, M.S.; Wei, H.X.; Paré, P.W.; Kloepper, J.W. Bacterial Volatiles Promote Growth in *Arabidopsis*. *Proc. Natl. Acad. Sci. USA* **2003**, *100*, 4927–4932. Erratum in *Proc. Natl. Acad. Sci. USA* **2003**, *100*, 8607. [CrossRef] [PubMed]
76. Glick, B.R. Bacteria with ACC Deaminase Can Promote Plant Growth and Help to Feed the World. *Microbiol. Res.* **2014**, *169*, 30–39. [CrossRef] [PubMed]
77. Gerke, J. Phytate (Inositol Hexakisphosphate) in Soil and Phosphate Acquisition from Inositol Phosphates by Higher Plants. A Review. *Plants* **2015**, *4*, 253–266. [CrossRef] [PubMed]
78. Keasling, J.D.; Bertsch, L.; Kornberg, A. Guanosine Pentaphosphate Phosphohydrolase of *Escherichia coli* Is a Long-Chain Exopolyphosphatase. *Proc. Natl. Acad. Sci. USA* **1993**, *90*, 7029–7033. [CrossRef] [PubMed]

79. Hone, H.; Li, T.; Wood, J.L.; Kaur, J.; Sawbridge, T. Transcriptome Analysis of *Pantoea rara* Mutants Reveals the Underlying Complexity of Bacterial Phosphate Solubilization. *Microbiol. Spectr.* **2026**, *14*, e03363-25. [CrossRef] [PubMed]
80. Rios-Galicia, B.; Villagómez-Garfias, C.; De la Vega-Camarillo, E.; Guerra-Camacho, J.E.; Medina-Jaritz, N.; Arteaga-Garibay, R.I.; Villa-Tanaca, L.; Hernández-Rodríguez, C. The Mexican Giant Maize of Jala Landrace Harbour Plant-Growth-Promoting Rhizospheric and Endophytic Bacteria. *3 Biotech* **2021**, *11*, 447. [CrossRef] [PubMed]
81. Dumigan, C.R.; Muileboom, J.; Gregory, J.; Shrestha, A.; Hewedy, O.A.; Raizada, M.N. Ancient Relatives of Modern Maize from the Center of Maize Domestication and Diversification Host Endophytic Bacteria That Confer Tolerance to Nitrogen Starvation. *Front. Plant Sci.* **2021**, *12*, 660673. [CrossRef] [PubMed]
82. Rivera-Hernández, G.; Tijerina-Castro, G.D.; Cortés-Pérez, S.; Ferrera-Cerrato, R.; Alarcón, A. Evaluation of Functional Plant Growth-Promoting Activities of Culturable Rhizobacteria Associated to Tunicate Maize (*Zea mays* var. *tunicata* A. St. Hil), a Mexican Exotic Landrace Grown in Traditional Agroecosystems. *Front. Microbiol.* **2024**, *15*, 1478807. [CrossRef] [PubMed]

Disclaimer/Publisher's Note: The statements, opinions and data contained in all publications are solely those of the individual author(s) and contributor(s) and not of MDPI and/or the editor(s). MDPI and/or the editor(s) disclaim responsibility for any injury to people or property resulting from any ideas, methods, instructions or products referred to in the content.